Comparison of cell-centered and node-centered formulations of a high-resolution well-balanced finite volume scheme: application to shallow water flows

Dr Argiris I. Delis

Dr Ioannis K. Nikolos (TUC)

Maria Kazolea (TUC)

Department of Sciences-Division of Mathematics

Technical University of Crete (TUC), Chania, Greece

By the words of Morton and Sonar (Acta Numerica, 2007):

"The jury was out there for a long time in the judgment between cell-center and vertex-center methods"

Overview

➜ The 2D nonlinear shallow water model

Overview

- The 2D nonlinear shallow water model
- Different grids and grid terminology used in this work

Overview

- The 2D nonlinear shallow water model
- Different grids and grid terminology used in this work
- Finite volumes on triangles: The node-center (NCFV) and cell-center (CCFV) approach, **in a unified framework**

Overview

- The 2D nonlinear shallow water model
- Different grids and grid terminology used in this work
- Finite volumes on triangles: The node-center (NCFV) and cell-center (CCFV) approach, **in a unified framework**
- Considerations and improved linear reconstruction for the CCFV approach

Overview

- The 2D nonlinear shallow water model
- Different grids and grid terminology used in this work
- Finite volumes on triangles: The node-center (NCFV) and cell-center (CCFV) approach, **in a unified framework**
- Considerations and improved linear reconstruction for the CCFV approach
- Topography discretisation and wet/dry front treatment.

Overview

- The 2D nonlinear shallow water model
- Different grids and grid terminology used in this work
- Finite volumes on triangles: The node-center (NCFV) and cell-center (CCFV) approach, **in a unified framework**
- Considerations and improved linear reconstruction for the CCFV approach
- Topography discretisation and wet/dry front treatment.
- Convergence tests, on different grids, for problems with known analytical solutions

Overview

- The 2D nonlinear shallow water model
- Different grids and grid terminology used in this work
- Finite volumes on triangles: The node-center (NCFV) and cell-center (CCFV) approach, **in a unified framework**
- Considerations and improved linear reconstruction for the CCFV approach
- Topography discretisation and wet/dry front treatment.
- Convergence tests, on different grids, for problems with known analytical solutions
- The Malpasset dam case

Overview

- The 2D nonlinear shallow water model
- Different grids and grid terminology used in this work
- Finite volumes on triangles: The node-center (NCFV) and cell-center (CCFV) approach, **in a unified framework**
- Considerations and improved linear reconstruction for the CCFV approach
- Topography discretisation and wet/dry front treatment.
- Convergence tests, on different grids, for problems with known analytical solutions
- The Malpasset dam case
- Conclusions

MATHEMATICAL MODEL: 2D Non-linear Shallow Water Equations

$$\frac{\partial \mathbf{U}}{\partial t} + \nabla \cdot \mathcal{F}(\mathbf{U}) = \mathcal{L}(\mathbf{U}, x, y) \quad \text{on} \quad \Omega \times [0, t] \subset \mathbb{R}^2 \times \mathbb{R}^+,$$

$$\mathbf{U} = \begin{bmatrix} h \\ hu \\ hv \end{bmatrix}, \quad \mathcal{F}(\mathbf{U}) = [\mathbf{F} \quad \mathbf{G}] = \begin{bmatrix} hu & hv \\ hu^2 + \frac{1}{2}gh^2 & huv \\ huv & hv^2 + \frac{1}{2}gh^2 \end{bmatrix},$$

$$\mathcal{L}(\mathbf{U}) = [\mathbf{R}^1 + \mathbf{R}^2 + \mathbf{S}]$$

$$\mathbf{R}^1 = \begin{bmatrix} 0 & -gh\frac{\partial B(x,y)}{\partial x} & 0 \end{bmatrix}^{\mathrm{T}} \quad \text{and} \quad \mathbf{R}^2 = \begin{bmatrix} 0 & 0 & -gh\frac{\partial B(x,y)}{\partial y} \end{bmatrix}^{\mathrm{T}} \text{ and}$$

$$\mathbf{S} = \begin{bmatrix} 0 & -ghS_f^x & -ghS_f^y \end{bmatrix}^{\mathrm{T}},$$

$$S_f^x = n_m^2 \frac{u\sqrt{u^2+v^2}}{h^{4/3}}, \quad S_f^y = n_m^2 \frac{v\sqrt{u^2+v^2}}{h^{4/3}}$$

Constructing Numerical Methods: Objectives

We need numerical schemes that are:

1. Conservative (conservation of physical quantities).

Constructing Numerical Methods: Objectives

We need numerical schemes that are:

1. Conservative (conservation of physical quantities).

2. Shock-Capturing with sharp non-oscillatory high-resolution of discontinuities.

Constructing Numerical Methods: Objectives

We need numerical schemes that are:

1. Conservative (conservation of physical quantities).
2. Shock-Capturing with sharp non-oscillatory high-resolution of discontinuities.
3. Converge to the correct physical solutions (entropy solutions).

Constructing Numerical Methods: Objectives

We need numerical schemes that are:

1. Conservative (conservation of physical quantities).

2. Shock-Capturing with sharp non-oscillatory high-resolution of discontinuities.

3. Converge to the correct physical solutions (entropy solutions).

4. At least second-order accurate on smooth regions of the flow.

Constructing Numerical Methods: Objectives

We need numerical schemes that are:

1. Conservative (conservation of physical quantities).

2. Shock-Capturing with sharp non-oscillatory high-resolution of discontinuities.

3. Converge to the correct physical solutions (entropy solutions).

4. At least second-order accurate on smooth regions of the flow.

5. Can handle complex topography and accurate predict wet/dry fronts.

Constructing Numerical Methods: Objectives

We need numerical schemes that are:

1. Conservative (conservation of physical quantities).

2. Shock-Capturing with sharp non-oscillatory high-resolution of discontinuities.

3. Converge to the correct physical solutions (entropy solutions).

4. At least second-order accurate on smooth regions of the flow.

5. Can handle complex topography and accurate predict wet/dry fronts.

6. Well-balanced between (numerical) fluxes and sources.

Constructing Numerical Methods: Objectives

We need numerical schemes that are:

1. Conservative (conservation of physical quantities).
2. Shock-Capturing with sharp non-oscillatory high-resolution of discontinuities.
3. Converge to the correct physical solutions (entropy solutions).
4. At least second-order accurate on smooth regions of the flow.
5. Can handle complex topography and accurate predict wet/dry fronts.
6. Well-balanced between (numerical) fluxes and sources.
7. Enable various practical inflow/outflow boundary conditions

Constructing Numerical Methods: Objectives

We need numerical schemes that are:

1. Conservative (conservation of physical quantities).
2. Shock-Capturing with sharp non-oscillatory high-resolution of discontinuities.
3. Converge to the correct physical solutions (entropy solutions).
4. At least second-order accurate on smooth regions of the flow.
5. Can handle complex topography and accurate predict wet/dry fronts.
6. Well-balanced between (numerical) fluxes and sources.
7. Enable various practical inflow/outflow boundary conditions
8. Preserve the positivity of the water depth.

Grid Terminilogy

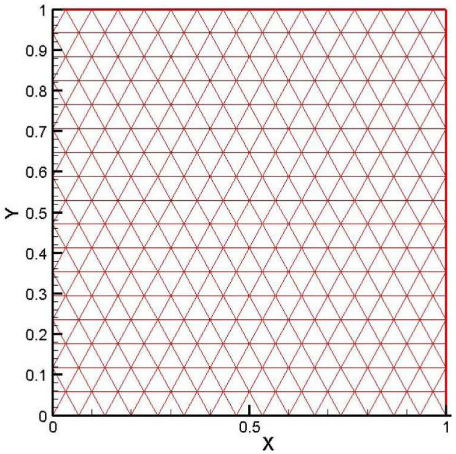

(a) Equilateral (Type-I)

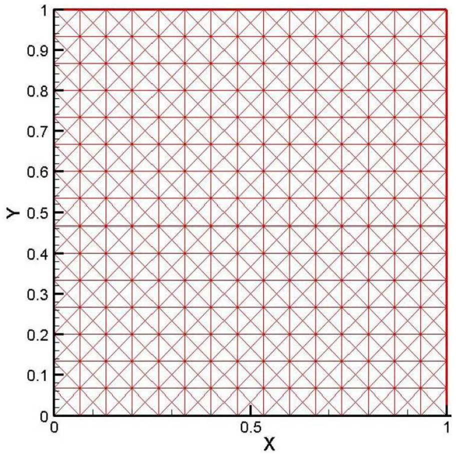

(b) Orthogonal (Type-II)

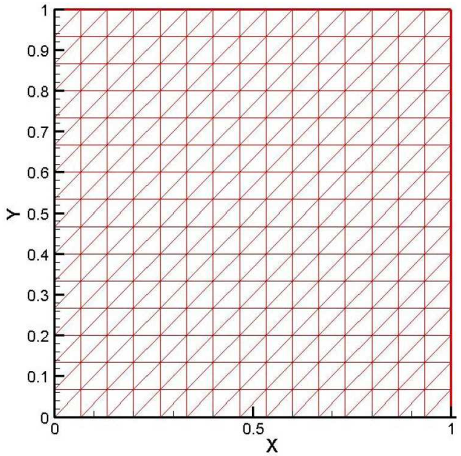

(c) Orthogonal (Type-III)

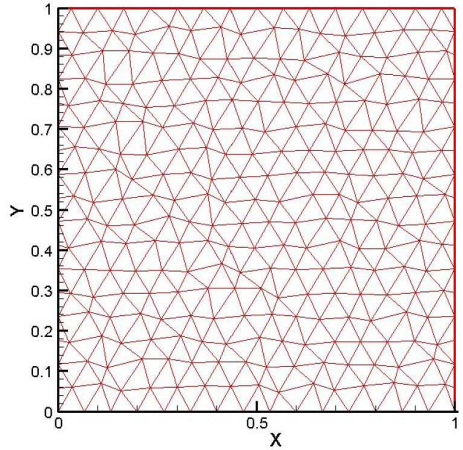

(d) Distorted (Type-IV)

Grid Terminilogy

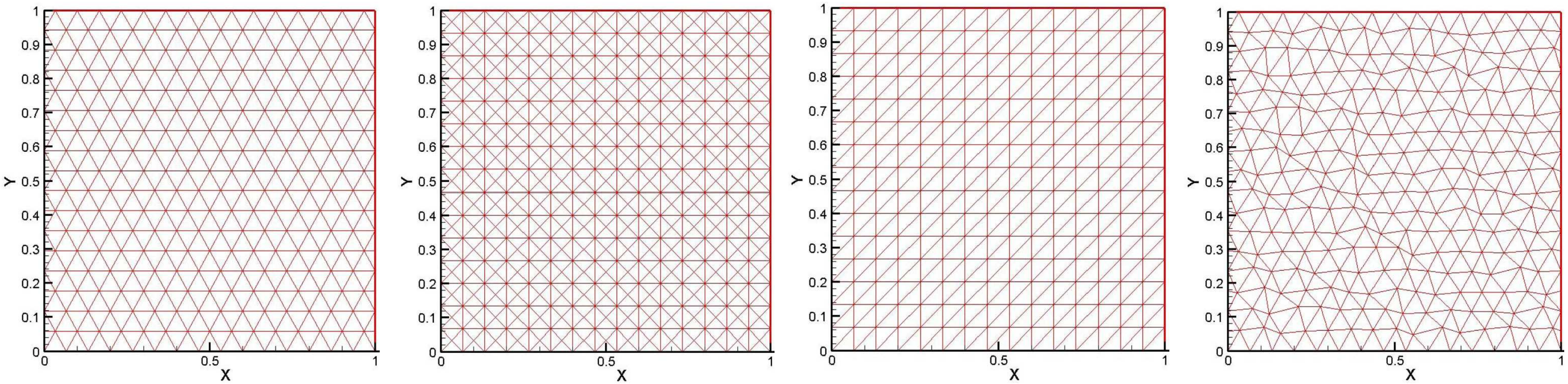

(a) Equilateral (Type-I) (b) Orthogonal (Type-II) (c) Orthogonal (Type-III) (d) Distorted (Type-IV)

➜ Major requirement: to enable meaningful asymptotic order of convergence use **consistently refined grids,** i.e. for $N =$ degrees of freedom, the characteristic length $h_N = \sqrt{(L_x \times L_y)/N}$,

Grid Terminilogy

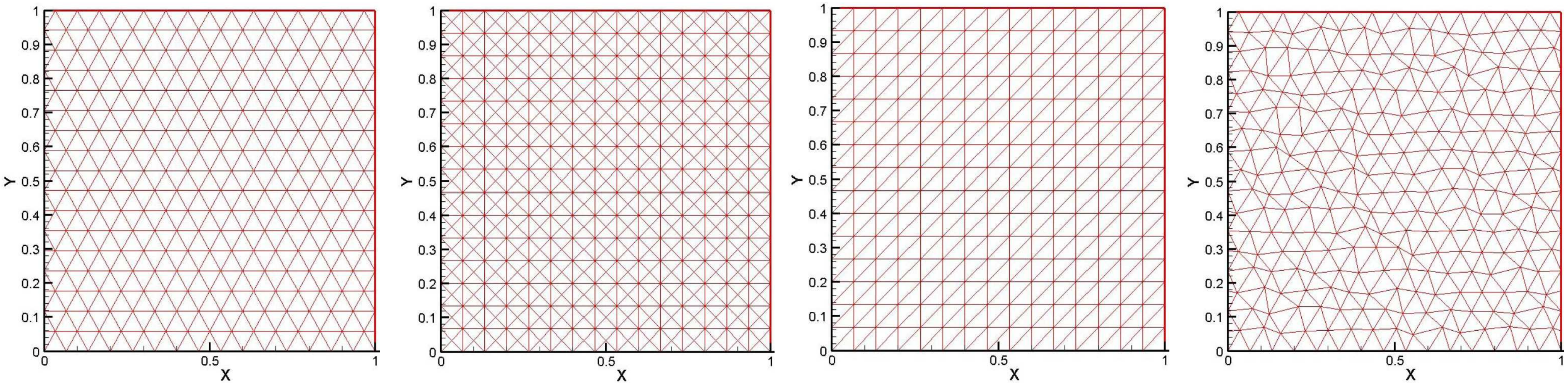

(a) Equilateral (Type-I) (b) Orthogonal (Type-II) (c) Orthogonal (Type-III) (d) Distorted (Type-IV)

- ➜ Major requirement: to enable meaningful asymptotic order of convergence use **consistently refined grids,** i.e. for $N =$ degrees of freedom, the characteristic length $h_N = \sqrt{(L_x \times L_y)/N}$,

- ➜ For fair comparison between NCFV and CCFV need to derive **equivalent meshes**, based on the degrees of freedom N,

Grid Terminilogy

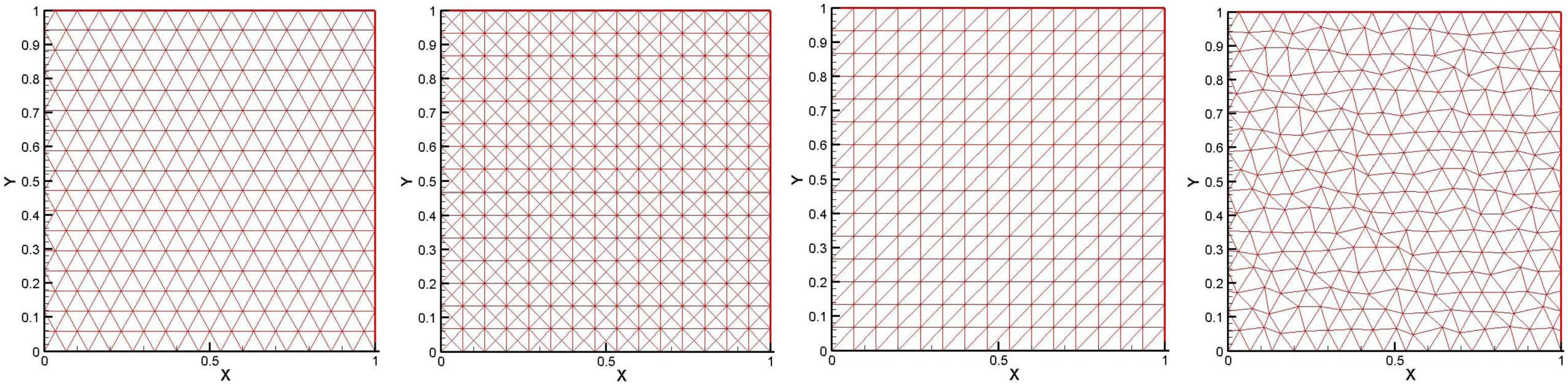

(a) Equilateral (Type-I) (b) Orthogonal (Type-II) (c) Orthogonal (Type-III) (d) Distorted (Type-IV)

- Major requirement: to enable meaningful asymptotic order of convergence use **consistently refined grids,** i.e. for $N =$ degrees of freedom, the characteristic length $h_N = \sqrt{(L_x \times L_y)/N}$,

- For fair comparison between NCFV and CCFV need to derive **equivalent meshes**, based on the degrees of freedom N,

- Measure the grid irregularity, e.g. use proper grid metrics.

FV discretization schemes on triangles: NCFV approach

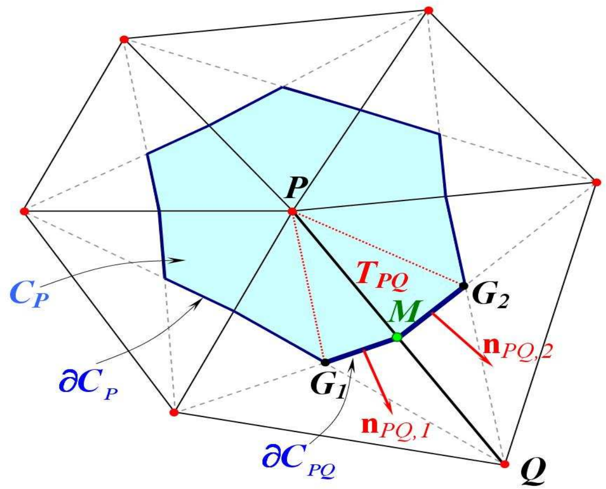

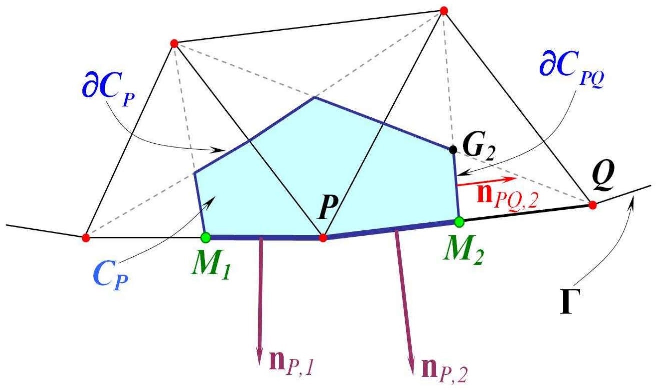

$$\iint_{C_P} \frac{\partial \mathbf{U}}{\partial t} dx dy + \oint_{\partial C_P} \left(\mathbf{F}\widetilde{n}_x + \mathbf{G}\widetilde{n}_y \right) dl = \iint_{C_P} \mathcal{L}\, dx dy$$

FV discretization schemes on triangles: NCFV approach

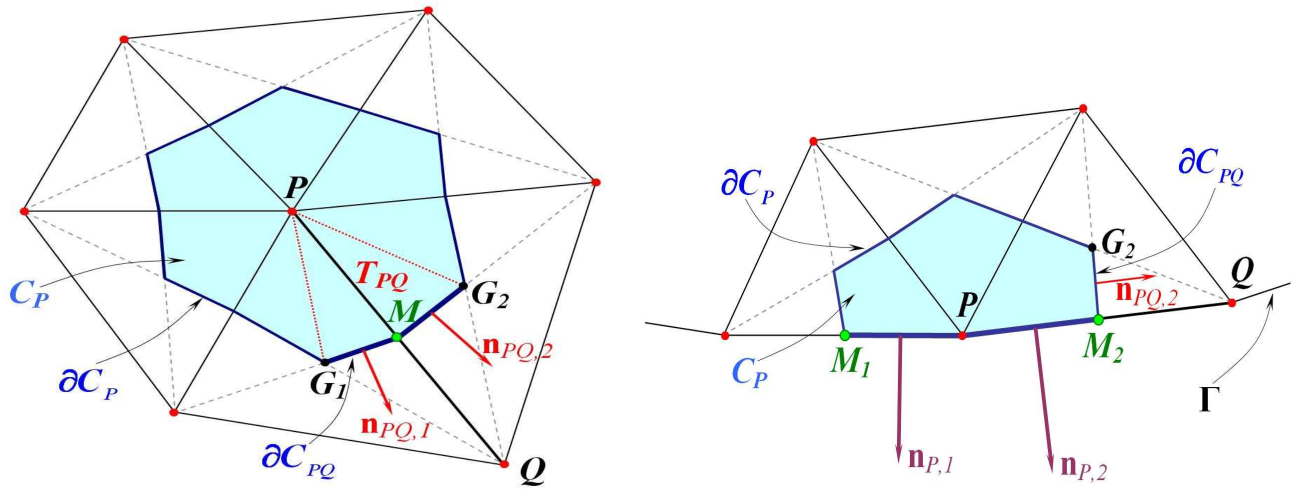

$$\iint_{C_P} \frac{\partial \mathbf{U}}{\partial t} dxdy + \oint_{\partial C_P} \left(\mathbf{F}\widetilde{n}_x + \mathbf{G}\widetilde{n}_y \right) dl = \iint_{C_P} \mathcal{L}\, dxdy$$

$$\frac{\partial \mathbf{U}_P}{\partial t}|C_P| + \sum_{Q\in K_P} \mathbf{\Phi}_{PQ} + \mathbf{\Phi}_{P,out} = \sum_{Q\in K_P} \left\{ \iint_{T_{PQ}.} \mathcal{L}\, dxdy \right\}$$ where

$$\mathbf{\Phi}_{PQ} = \mathbf{Z}\left(\mathbf{U}^L_{PQ}, \mathbf{n}_{PQ}\right) + \widetilde{\mathbf{J}}^-_{PQ}\left(\mathbf{U}^R_{PQ} - \mathbf{U}^L_{PQ}\right),$$ with $$\widetilde{\mathbf{J}}^-_{PQ} = \left(\widetilde{\mathbf{P}}\widetilde{\mathbf{\Lambda}}^-\widetilde{\mathbf{P}}^{-1}\right)_{PQ},$$

$\mathbf{\Phi}_{PQ}$ is the **Roe numerical flux**, evaluated at $\mathbf{U}^L_{PQ}$ and $\mathbf{U}^R_{PQ}$ **reconstructed** values.

For MUSCL $(\nabla \mathbf{W})_P$ has to be computed in each dual cell P

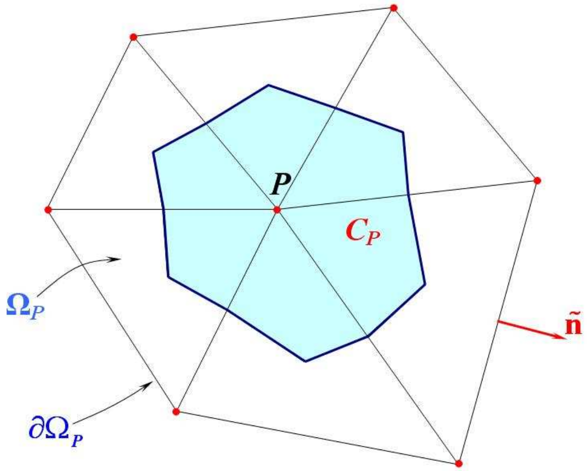

Green-Gauss (G-G) linear reconstruction

$$(\nabla w_i)_P = \frac{1}{|C_P|} \sum_{Q \in K_P} \frac{1}{2}\Big(w_{i,P} + w_{i,Q}\Big)\mathbf{n}_{PQ}.$$

$$w^L_{i,PQ} = w_{i,P} + \frac{1}{2}\text{LIM}\left((\nabla w_i)_P^{\text{upw}} \cdot \mathbf{r}_{PQ}, (\nabla w_i)^{\text{cent}} \cdot \mathbf{r}_{PQ}\right);$$

$$w^R_{i,PQ} = w_{i,Q} - \frac{1}{2}\text{LIM}\left((\nabla w_i)_Q^{\text{upw}} \cdot \mathbf{r}_{PQ}, (\nabla w_i)^{\text{cent}} \cdot \mathbf{r}_{PQ}\right),$$

For MUSCL $(\nabla \mathbf{W})_P$ has to be computed in each dual cell P

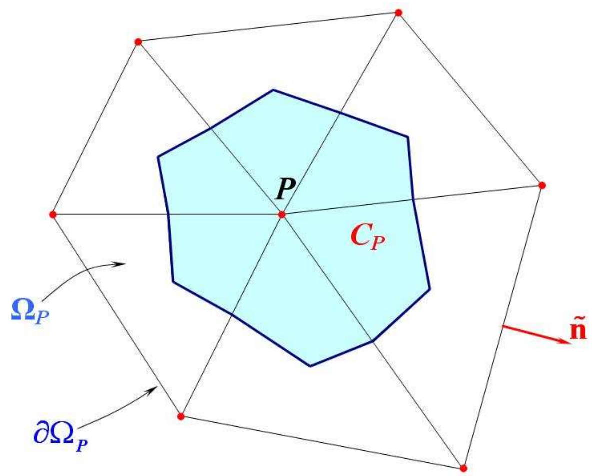

Green-Gauss (G-G) linear reconstruction

$$(\nabla w_i)_P = \frac{1}{|C_P|} \sum_{Q \in K_P} \frac{1}{2}\Big(w_{i,P} + w_{i,Q}\Big)\mathbf{n}_{PQ}.$$

$$w^L_{i,PQ} = w_{i,P} + \frac{1}{2}\text{LIM}\left((\nabla w_i)^{\text{upw}}_P \cdot \mathbf{r}_{PQ}, (\nabla w_i)^{\text{cent}} \cdot \mathbf{r}_{PQ}\right);$$

$$w^R_{i,PQ} = w_{i,Q} - \frac{1}{2}\text{LIM}\left((\nabla w_i)^{\text{upw}}_Q \cdot \mathbf{r}_{PQ}, (\nabla w_i)^{\text{cent}} \cdot \mathbf{r}_{PQ}\right),$$

$$(\nabla w_i)^{\text{cent}} \cdot \mathbf{r}_{PQ} = w_{i,Q} - w_{i,P}, \quad (\nabla w_i)^{\text{upw}}_P = 2\,(\nabla w_i)_P - (\nabla w_i)^{\text{cent}}$$

For MUSCL $(\nabla \mathbf{W})_P$ has to be computed in each dual cell P

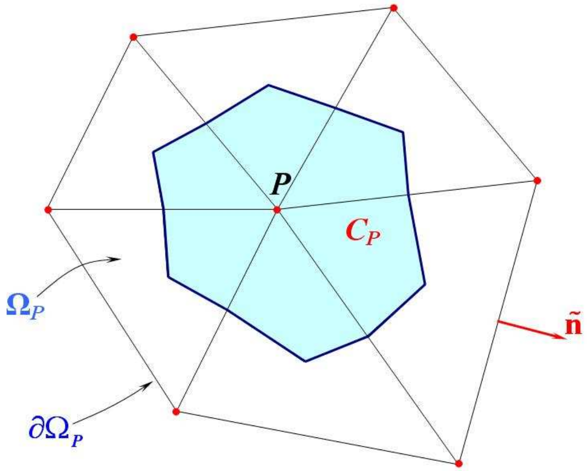

Green-Gauss (G-G) linear reconstruction

$$(\nabla w_i)_P = \frac{1}{|C_P|} \sum_{Q \in K_P} \frac{1}{2}\Big(w_{i,P} + w_{i,Q}\Big)\mathbf{n}_{PQ}.$$

$$w^L_{i,PQ} = w_{i,P} + \frac{1}{2}\text{LIM}\left((\nabla w_i)_P^{\text{upw}} \cdot \mathbf{r}_{PQ}, (\nabla w_i)^{\text{cent}} \cdot \mathbf{r}_{PQ}\right);$$

$$w^R_{i,PQ} = w_{i,Q} - \frac{1}{2}\text{LIM}\left((\nabla w_i)_Q^{\text{upw}} \cdot \mathbf{r}_{PQ}, (\nabla w_i)^{\text{cent}} \cdot \mathbf{r}_{PQ}\right),$$

$$(\nabla w_i)^{\text{cent}} \cdot \mathbf{r}_{PQ} = w_{i,Q} - w_{i,P}, \quad (\nabla w_i)_P^{\text{upw}} = 2\,(\nabla w_i)_P - (\nabla w_i)^{\text{cent}}$$

- Monotonicity in the reconstruction is enforced by using van Albada-van Leer **edge-based** slope limiter.

For MUSCL $(\nabla \mathbf{W})_P$ has to be computed in each dual cell P

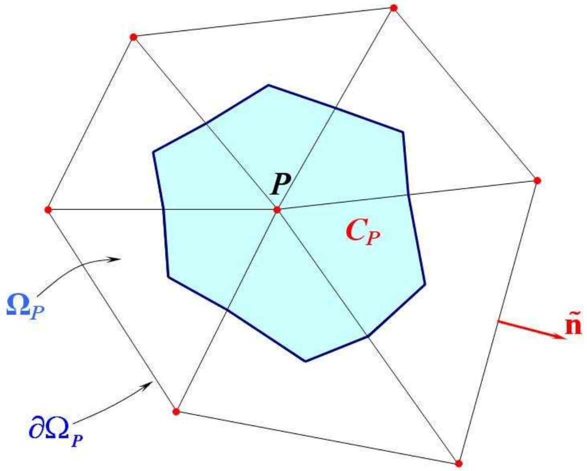

Green-Gauss (G-G) linear reconstruction

$$(\nabla w_i)_P = \frac{1}{|C_P|} \sum_{Q \in K_P} \frac{1}{2}\Big(w_{i,P} + w_{i,Q}\Big)\mathbf{n}_{PQ}.$$

$$w^L_{i,PQ} = w_{i,P} + \frac{1}{2}\text{LIM}\left((\nabla w_i)_P^{\text{upw}} \cdot \mathbf{r}_{PQ}, (\nabla w_i)^{\text{cent}} \cdot \mathbf{r}_{PQ}\right);$$

$$w^R_{i,PQ} = w_{i,Q} - \frac{1}{2}\text{LIM}\left((\nabla w_i)_Q^{\text{upw}} \cdot \mathbf{r}_{PQ}, (\nabla w_i)^{\text{cent}} \cdot \mathbf{r}_{PQ}\right),$$

$$(\nabla w_i)^{\text{cent}} \cdot \mathbf{r}_{PQ} = w_{i,Q} - w_{i,P}, \quad (\nabla w_i)_P^{\text{upw}} = 2\,(\nabla w_i)_P - (\nabla w_i)^{\text{cent}}$$

- Monotonicity in the reconstruction is enforced by using van Albada-van Leer **edge-based** slope limiter.
- The same reconstruction is used to compute the gradient for $B(x, y)$.

FV discretization schemes on triangles: CCFV approach

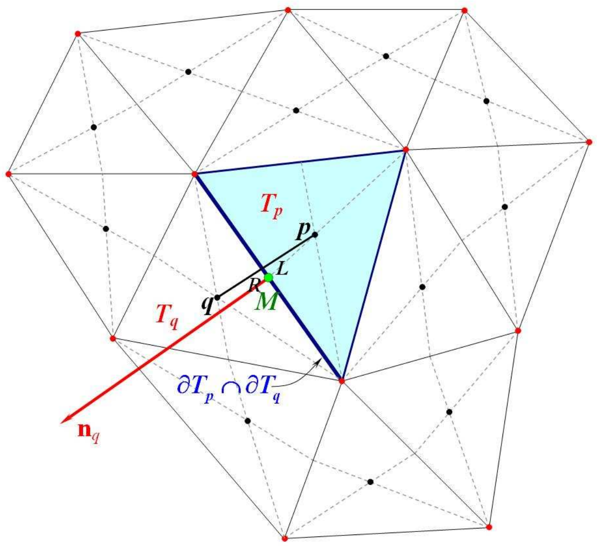

$$\frac{\partial \mathbf{U}_p}{\partial t}|T_p| = \sum_{q \in K(p)} \mathbf{\Phi}_q + \iint_{T_p} \mathcal{L} d\Omega.$$

With the usual one
point quadrature at M, Roe's solver is again utilized

$$\mathbf{\Phi}_q = \mathbf{Z}\left(\mathbf{U}_p^L, \mathbf{n}_q\right) + \widetilde{\mathbf{J}}_{LR}^{-}\Big(\mathbf{U}_q^R - \mathbf{U}_p^L\Big).$$

FV discretization schemes on triangles: CCFV approach

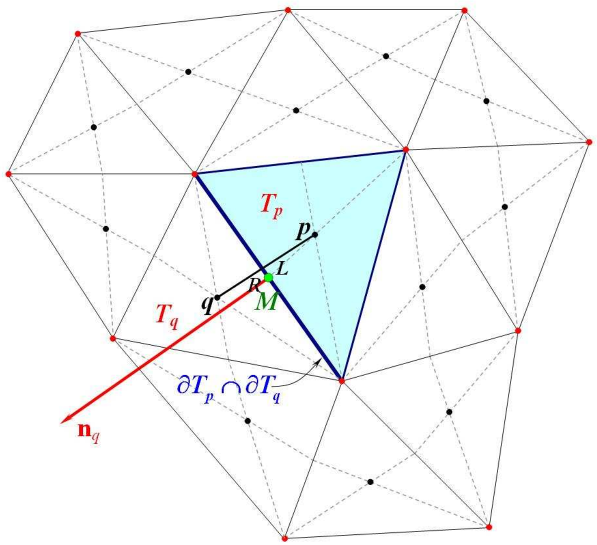

$$\frac{\partial \mathbf{U}_p}{\partial t}|T_p| = \sum_{q \in K(p)} \mathbf{\Phi}_q + \iint_{T_p} \mathcal{L} d\Omega.$$

With the usual one
point quadrature at M, Roe's solver is again utilized

$$\mathbf{\Phi}_q = \mathbf{Z}\left(\mathbf{U}_p^L, \mathbf{n}_q\right) + \widetilde{\mathbf{J}}_{LR}^{-}\Big(\mathbf{U}_q^R - \mathbf{U}_p^L\Big).$$

Linear reconstruction for the CCFV scheme

- Naive calculation (at point D)

$$(w_{i,p})_D^L = w_{i,p} + \frac{||\mathbf{r}_{pD}||}{||\mathbf{r}_{pq}||}\text{LIM}\left((\nabla w_i)_p^{\text{upw}} \cdot \mathbf{r}_{pq}, (\nabla w_i)^{\text{cent}} \cdot \mathbf{r}_{pq}\right);$$

$$(w_{i,q})_D^R = w_{i,q} - \frac{||\mathbf{r}_{Dq}||}{||\mathbf{r}_{pq}||}\text{LIM}\left((\nabla w_i)_q^{\text{upw}} \cdot \mathbf{r}_{pq}, (\nabla w_i)^{\text{cent}} \cdot \mathbf{r}_{pq}\right)$$

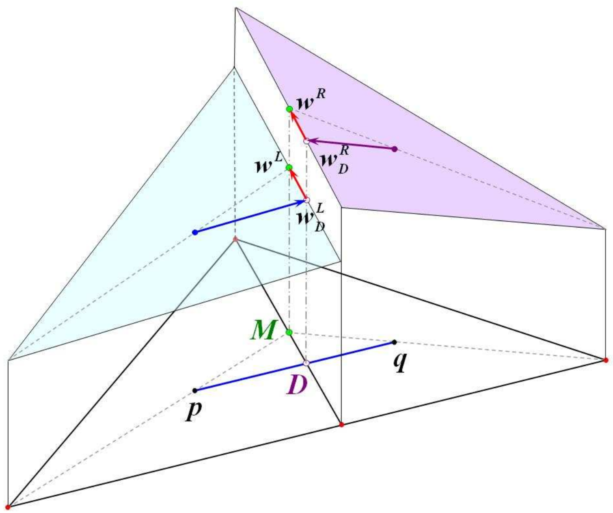

FV discretization schemes on triangles: CCFV approach

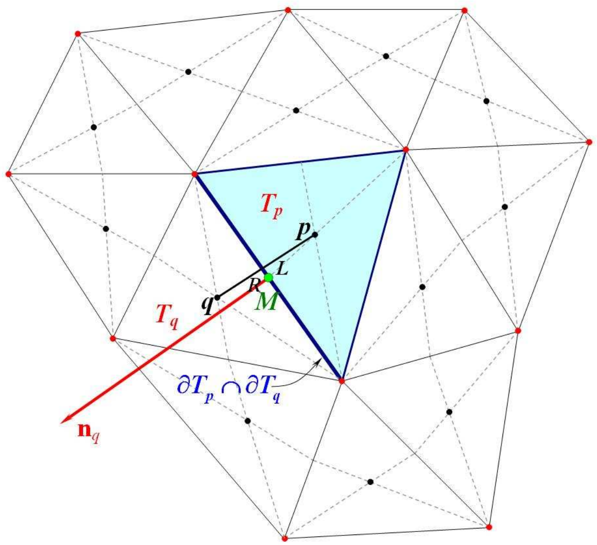

$$\frac{\partial \mathbf{U}_p}{\partial t}|T_p| = \sum_{q\in K(p)} \mathbf{\Phi}_q + \iint_{T_p} \mathcal{L} d\Omega.$$

With the usual one
point quadrature at M, Roe's solver is again utilized

$$\mathbf{\Phi}_q = \mathbf{Z}\left(\mathbf{U}_p^L, \mathbf{n}_q\right) + \widetilde{\mathbf{J}}_{LR}^{-}\Big(\mathbf{U}_q^R - \mathbf{U}_p^L\Big).$$

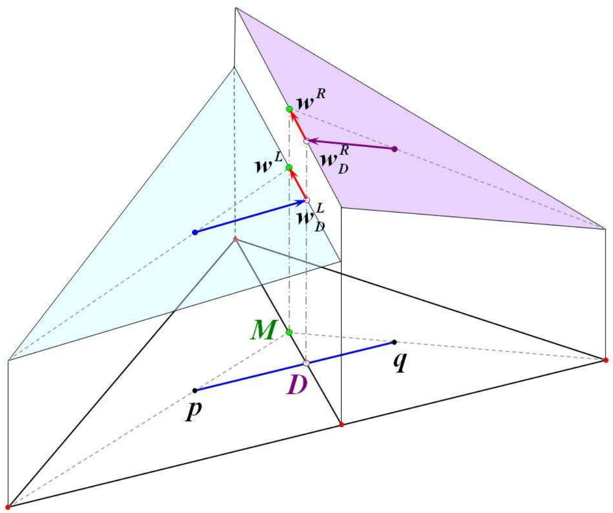

Linear reconstruction for the CCFV scheme

- Naive calculation (at point D)

$$(w_{i,p})_D^L = w_{i,p} + \frac{||\mathbf{r}_{pD}||}{||\mathbf{r}_{pq}||}\text{LIM}\left((\nabla w_i)_p^{\text{upw}}\cdot \mathbf{r}_{pq}, (\nabla w_i)^{\text{cent}}\cdot \mathbf{r}_{pq}\right);$$

$$(w_{i,q})_D^R = w_{i,q} - \frac{||\mathbf{r}_{Dq}||}{||\mathbf{r}_{pq}||}\text{LIM}\left((\nabla w_i)_q^{\text{upw}}\cdot \mathbf{r}_{pq}, (\nabla w_i)^{\text{cent}}\cdot \mathbf{r}_{pq}\right)$$

- Corrected calculation (at point M)

$$w_{i,p}^L = (w_{i,p})_D^L + \mathbf{r}_{DM}\cdot(\nabla w_i)_p,$$
$$w_{i,q}^R = (w_{i,q})_D^R + \mathbf{r}_{DM}\cdot(\nabla w_i)_q.$$

CCFV approach: Gradient operators

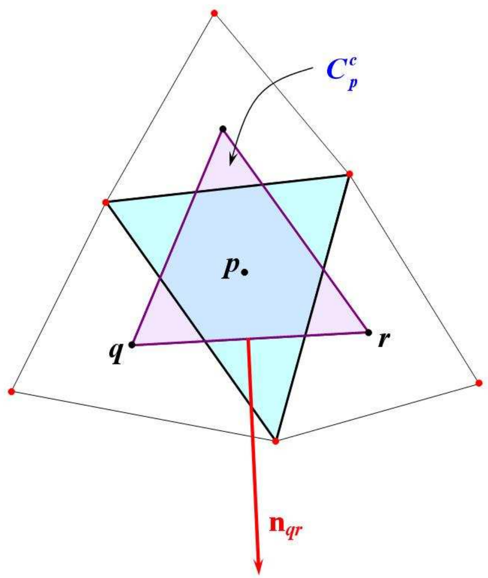

Three element (compact stencil) gradient

$$\nabla w_{i,p} = \frac{1}{|C_p^c|} \sum_{\substack{q,r \in K(p) \\ r \neq q}} \frac{1}{2}\Big(w_{i,q} + w_{i,r}\Big)\mathbf{n}_{qr}.$$

CCFV approach: Gradient operators

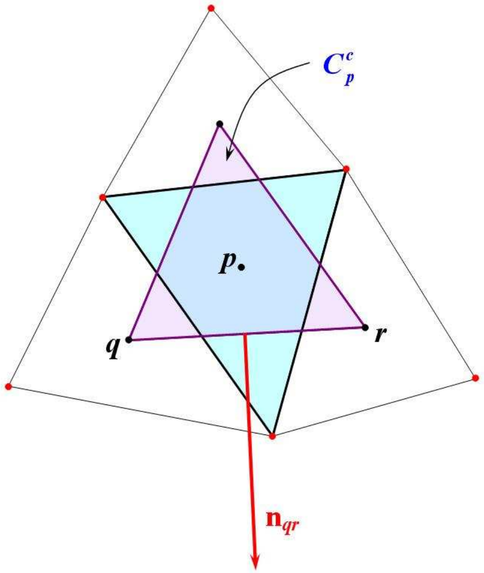

Three element (compact stencil) gradient

$$\nabla w_{i,p} = \frac{1}{|C_p^c|} \sum_{\substack{q,r \in K(p) \\ r \neq q}} \frac{1}{2}\Big(w_{i,q} + w_{i,r}\Big)\mathbf{n}_{qr}.$$

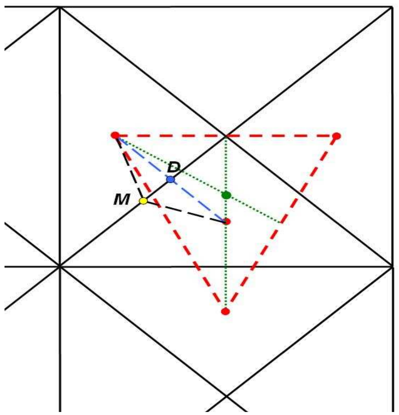

CCFV approach: Gradient operators

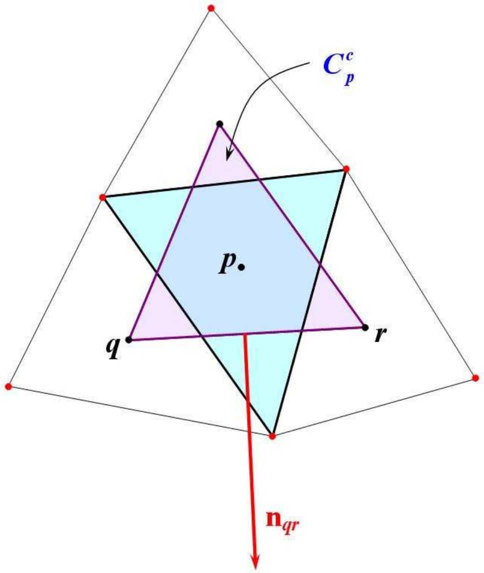

Three element (compact stencil) gradient

$$\nabla w_{i,p} = \frac{1}{|C_p^c|} \sum_{\substack{q,r \in K(p) \\ r \neq q}} \frac{1}{2}\Big(w_{i,q} + w_{i,r}\Big)\mathbf{n}_{qr}.$$

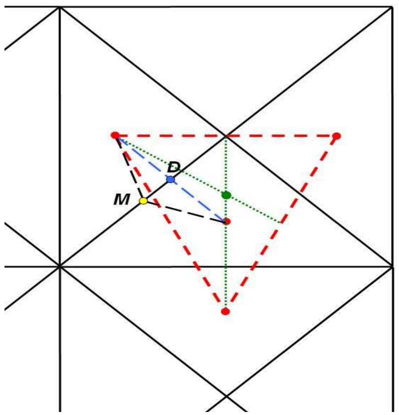

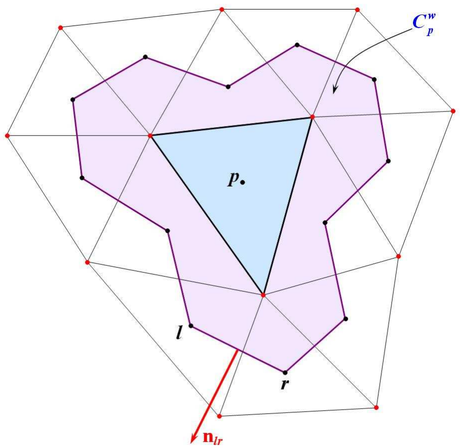

Extended element (wide stencil) gradient

$$\nabla w_{i,p} = \frac{1}{|C_p^w|} \sum_{\substack{l,r \in K'(p) \\ r \neq l}} \frac{1}{2}\Big(w_{i,l} + w_{i,r}\Big)\mathbf{n}_{lr}$$

Typical behavior of the CCFV scheme at internal and boundary faces

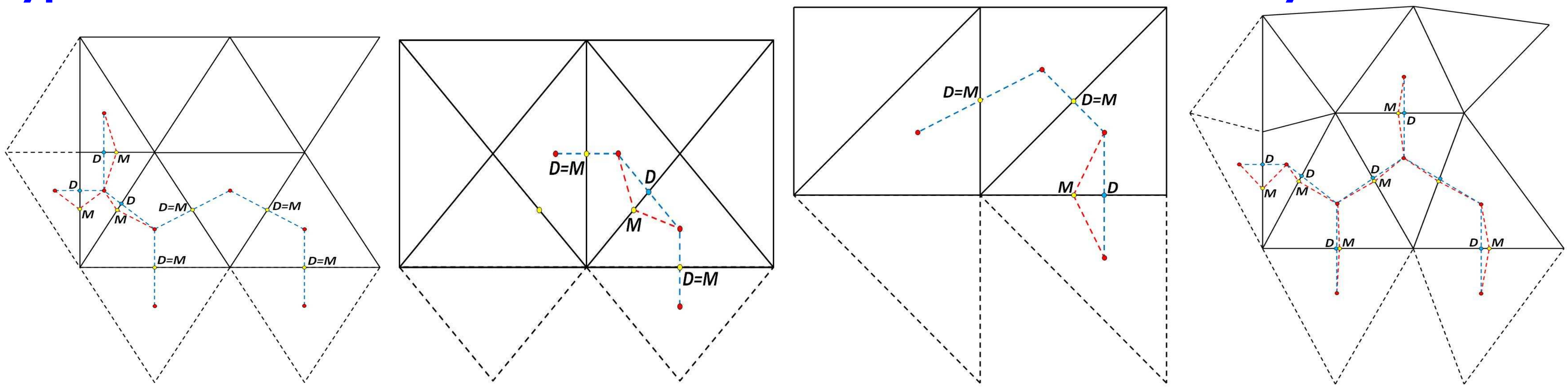

- Keeping in mind that, we want to apply the same edge-based limiter as for the NCFV scheme

Typical behavior of the CCFV scheme at internal and boundary faces

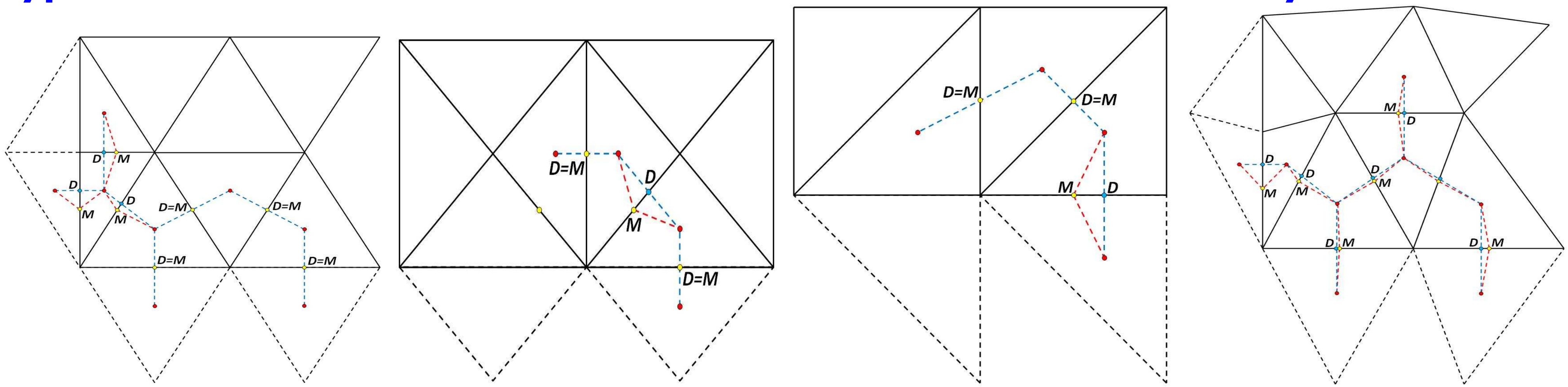

- Keeping in mind that, we want to apply the same edge-based limiter as for the NCFV scheme
- In an ideal unstructured grid, variables are extrapolated at M which will coincide with D (intersection point of face $\partial T_q \cap \partial T_p$ and $\overline{pq}$).

Typical behavior of the CCFV scheme at internal and boundary faces

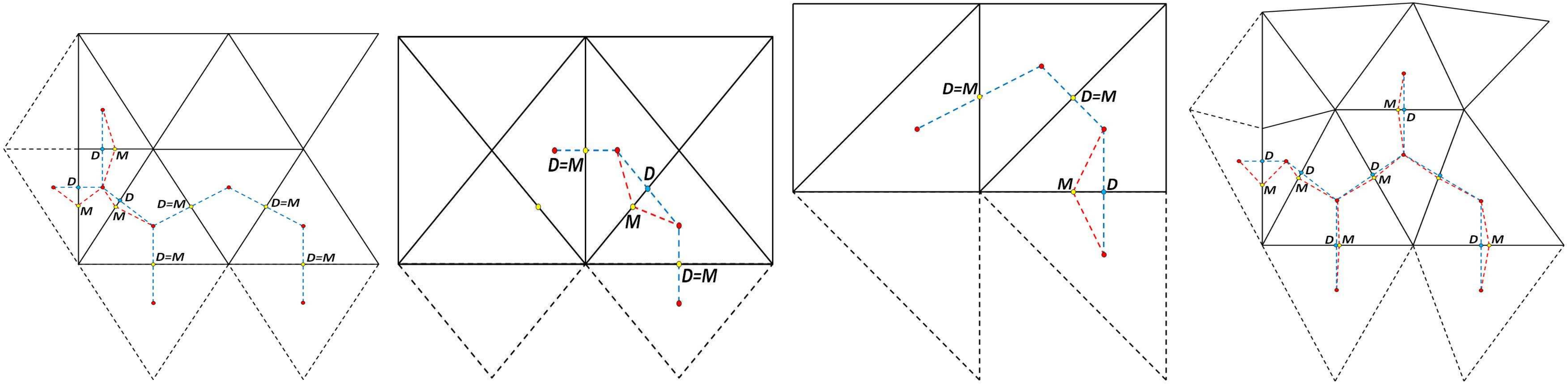

- Keeping in mind that, we want to apply the same edge-based limiter as for the NCFV scheme
- In an ideal unstructured grid, variables are extrapolated at M which will coincide with D (intersection point of face $\partial T_q \cap \partial T_p$ and $\overline{pq}$).
- There can be a "large" distance between M and D (also on boundary faces, where ghost cells are used).

Topography source discretization (wet/wet case)

➜ C-property: (Bermudez and Vazquez, 1994)

A numerical should resolve exactly steady-state cases where:

$$u = v \equiv 0, \quad B^R - B^L = -(h^R - h^L).$$

Topography source discretization (wet/wet case)

- C-property: (Bermudez and Vazquez, 1994)

  A numerical should resolve exactly steady-state cases where:

$$u = v \equiv 0, \quad B^R - B^L = -(h^R - h^L).$$

- Upwind of the numerical source contribution to cell-i as

$$\widetilde{\mathbf{\Psi}}^- = \frac{1}{2}\left(\widetilde{\mathbf{P}}\left(\mathbf{I} - \left|\widetilde{\mathbf{\Lambda}}\right|\widetilde{\mathbf{\Lambda}}^{-1}\right)\widetilde{\mathbf{P}}^{-1}\widetilde{\mathbf{R}}\right)$$

Topography source discretization (wet/wet case)

- C-property: (Bermudez and Vazquez, 1994)

  A numerical should resolve exactly steady-state cases where:

$$u = v \equiv 0, \quad B^R - B^L = -(h^R - h^L).$$

- Upwind of the numerical source contribution to cell-i as

$$\widetilde{\mathbf{\Psi}}^- = \frac{1}{2}\left(\widetilde{\mathbf{P}}\left(\mathbf{I} - \left|\widetilde{\mathbf{\Lambda}}\right|\widetilde{\mathbf{\Lambda}}^{-1}\right)\widetilde{\mathbf{P}}^{-1}\widetilde{\mathbf{R}}\right)$$

- Satisfies the discrete steady state if $B^R = B_j$ and $B^L = B_i$ (1st order scheme):

$$\mathbf{Z}\left(\mathbf{U}^L, \mathbf{n}\right) + \widetilde{\mathbf{J}}^-\left(\mathbf{U}^R - \mathbf{U}^L\right) = \left(\frac{1}{2}\widetilde{\mathbf{P}}\left(\mathbf{I} - \left|\widetilde{\mathbf{\Lambda}}\right|\widetilde{\mathbf{\Lambda}}^{-1}\right)\widetilde{\mathbf{P}}^{-1}\widetilde{\mathbf{R}}\right)$$

Topography source discretization (wet/wet case)

- C-property: (Bermudez and Vazquez, 1994)

  A numerical should resolve exactly steady-state cases where:

$$u = v \equiv 0, \quad B^R - B^L = -(h^R - h^L).$$

- Upwind of the numerical source contribution to cell-i as

$$\widetilde{\boldsymbol{\Psi}}^- = \frac{1}{2}\left(\widetilde{\mathbf{P}}\left(\mathbf{I} - \left|\widetilde{\boldsymbol{\Lambda}}\right|\widetilde{\boldsymbol{\Lambda}}^{-1}\right)\widetilde{\mathbf{P}}^{-1}\widetilde{\mathbf{R}}\right)$$

- Satisfies the discrete steady state if $B^R = B_j$ and $B^L = B_i$ (1st order scheme):

$$\mathbf{Z}\left(\mathbf{U}^L, \mathbf{n}\right) + \widetilde{\mathbf{J}}^-\left(\mathbf{U}^R - \mathbf{U}^L\right) = \left(\frac{1}{2}\widetilde{\mathbf{P}}\left(\mathbf{I} - \left|\widetilde{\boldsymbol{\Lambda}}\right|\widetilde{\boldsymbol{\Lambda}}^{-1}\right)\widetilde{\mathbf{P}}^{-1}\widetilde{\mathbf{R}}\right)$$

when

$$\widetilde{\mathbf{R}} = \begin{bmatrix} 0 \\ -g\dfrac{h^L + h^R}{2}\left(B^R - B^L\right) n_x \\ -g\dfrac{h^L + h^R}{2}\left(B^R - B^L\right) n_y \end{bmatrix}$$

but in the 2nd order MUSCL discretization a **correction term** should be added to the source term $\widetilde{\boldsymbol{\Psi}}^{-}$ (Hubbard and Garcia-Navarro, 2000), i.e.

$$\begin{bmatrix} 0 \\ -g\dfrac{h^L + h_i}{2}\left(B^L - B_i\right) n_x \\ -g\dfrac{h^L + h_i}{2}\left(B^L - B_i\right) n_y \end{bmatrix}.$$

but in the 2nd order MUSCL discretization a **correction term** should be added to the source term $\widetilde{\boldsymbol{\Psi}}^-$ (Hubbard and Garcia-Navarro, 2000), i.e.

$$\begin{bmatrix} 0 \\ -g\dfrac{h^L + h_i}{2}\left(B^L - B_i\right) n_x \\ -g\dfrac{h^L + h_i}{2}\left(B^L - B_i\right) n_y \end{bmatrix}.$$

- the above term vanishes if $B^L = B_i$, i.e. 1st order schemes but in the 2nd order MUSCL discretization a **correction term** should be added to the source term $\widetilde{\mathbf{\Psi}}^-$ (Hubbard and Garcia-Navarro, 2000), i.e.

$$\begin{bmatrix} 0 \\ -g\dfrac{h^L + h_i}{2}\left(B^L - B_i\right) n_x \\ -g\dfrac{h^L + h_i}{2}\left(B^L - B_i\right) n_y \end{bmatrix}.$$

- the above term vanishes if $B^L = B_i$, i.e. 1st order schemes
- for hydrostatic (steady) conditions inside each cell-i

$$B^L - B_i = -\left(h^L - h_i\right)$$

but in the 2nd order MUSCL discretization a **correction term** should be added to the source term $\widetilde{\mathbf{\Psi}}^-$ (Hubbard and Garcia-Navarro, 2000), i.e.

$$\begin{bmatrix} 0 \\ -g\dfrac{h^L + h_i}{2}\left(B^L - B_i\right) n_x \\ -g\dfrac{h^L + h_i}{2}\left(B^L - B_i\right) n_y \end{bmatrix}.$$

- the above term vanishes if $B^L = B_i$, i.e. 1st order schemes
- for hydrostatic (steady) conditions inside each cell-i

$$B^L - B_i = -\left(h^L - h_i\right)$$

But what about wet/dry fronts and flow over adverse slopes?

Topography source discretization (wet/dry case)

- Extended C-property, (Castro et al., 2005)

  A scheme is considered to be well-balanced if it can solve exactly steady-state solutions corresponding to flow at rest, regardless of including wet/dry transitions or not.

- In the MUSCL scheme for hydrostatic conditions we must have, at $i-$cell

Topography source discretization (wet/dry case)

- Extended C-property, (Castro et al., 2005)

  A scheme is considered to be well-balanced if it can solve exactly steady-state solutions corresponding to flow at rest, regardless of including wet/dry transitions or not.

- In the MUSCL scheme for hydrostatic conditions we must have, at $i-$cell

  $$B^L - B_i = -\left(h^L - h_i\right)$$

Topography source discretization (wet/dry case)

➜ Extended C-property, (Castro et al., 2005)

A scheme is considered to be well-balanced if it can solve exactly steady-state solutions corresponding to flow at rest, regardless of including wet/dry transitions or not.

➜ In the MUSCL scheme for hydrostatic conditions we must have, at $i-$cell

$$B^L - B_i = -\left(h^L - h_i\right) \implies \quad (\nabla B)_i = -(\nabla h)_i$$

Topography source discretization (wet/dry case)

- Extended C-property, (Castro et al., 2005)

  A scheme is considered to be well-balanced if it can solve exactly steady-state solutions corresponding to flow at rest, regardless of including wet/dry transitions or not.

- In the MUSCL scheme for hydrostatic conditions we must have, at $i-$cell

$$B^L - B_i = -\left(h^L - h_i\right) \implies \quad (\nabla B)_i = -(\nabla h)_i$$

and similar for the $j-$cell $\implies \quad (\nabla B)_j = -(\nabla h)_j$

Topography source discretization (wet/dry case)

- Extended C-property, (Castro et al., 2005)

  A scheme is considered to be well-balanced if it can solve exactly steady-state solutions corresponding to flow at rest, regardless of including wet/dry transitions or not.

- In the MUSCL scheme for hydrostatic conditions we must have, at $i-$cell

  $$B^L - B_i = -\left(h^L - h_i\right) \implies \quad (\nabla B)_i = -(\nabla h)_i$$

  and similar for the $j-$cell $\implies \quad (\nabla B)_j = -(\nabla h)_j$

  If in the gradient calculation, of a wet cell, a dry node is involved we correct the h^L and/or h^R by imposing

Topography source discretization (wet/dry case)

- **Extended C-property**, (Castro et al., 2005)

  A scheme is considered to be well-balanced if it can solve exactly steady-state solutions corresponding to flow at rest, regardless of including wet/dry transitions or not.

- In the MUSCL scheme for hydrostatic conditions we must have, at $i-$cell

$$B^L - B_i = -\left(h^L - h_i\right) \implies \quad (\nabla B)_i = -(\nabla h)_i$$

and similar for the $j-$cell $\implies \quad (\nabla B)_j = -(\nabla h)_j$

If in the gradient calculation, of a wet cell, a dry node is involved we correct the h^L and/or h^R by imposing

$$h^L = h_i - (B^L - B_i) \qquad \textbf{and/or} \qquad h^R = h_j - (B^R - B_j)$$

Topography source discretization (wet/dry case)

- Extended C-property, (Castro et al., 2005)

  A scheme is considered to be well-balanced if it can solve exactly steady-state solutions corresponding to flow at rest, regardless of including wet/dry transitions or not.

- In the MUSCL scheme for hydrostatic conditions we must have, at $i-$cell

  $$B^L - B_i = -\left(h^L - h_i\right) \Longrightarrow \quad \left(\nabla B\right)_i = -\left(\nabla h\right)_i$$

  and similar for the $j-$cell $\Longrightarrow \quad \left(\nabla B\right)_j = -\left(\nabla h\right)_j$

  If in the gradient calculation, of a wet cell, a dry node is involved we correct the h^L and/or h^R by imposing

  $$h^L = h_i - (B^L - B_i) \qquad \textbf{and/or} \qquad h^R = h_j - (B^R - B_j)$$

- For emerging bed situations, in the dry $i-$node (cell), the bed value has to be redefined (Brufau et al., 2002) in $\widetilde{\mathbf{R}}$ and in order to maintain hydrostatic conditions i.e.

  $$\Delta B = \begin{cases} -(h^R - h^L), & \text{if } h^L > \varepsilon_{wd},\ h^R \leq \varepsilon_{wd} \text{ and } h^R < (B^R - B^L), \\ (B^L - B^R), & \text{otherwise.} \end{cases}$$

Solving at wet/dry front interface (continued)

For water in motion over emerging slopes, (Castro et al., 2005)

➜ A further assumption is made for a flow in motion over a slope

Solving at wet/dry front interface (continued)

For water in motion over emerging slopes, (Castro et al., 2005)

➜ A further assumption is made for a flow in motion over a slope

If $h^L > \varepsilon_{wd}$ and $h^R \leq \varepsilon_{wd}$ and $h^L < (B^R - B^L)$, then set **temporarily for the wet cell-i**

$$u^L = v^L = 0$$

➜ Then calculate the well-balanced MUSCL numerical fluxes and sources.

Solving at wet/dry front interface (continued)

For water in motion over emerging slopes, (Castro et al., 2005)

- A further assumption is made for a flow in motion over a slope

  If $h^L > \varepsilon_{wd}$ and $h^R \leq \varepsilon_{wd}$ and $h^L < (B^R - B^L)$, then set **temporarily for the wet cell-i**

$$u^L = v^L = 0$$

- Then calculate the well-balanced MUSCL numerical fluxes and sources.

- Finally in case of steep downhill slopes, h in wet cells may become negative. We apply the conservative approach of Brufau et. al. (2004) to **control negative depths** and **conserve mass**.

Other implementation details:

- **Dry cell identification:** use a wet/dry tolerance parameter ε_{wd} depending on grid characteristics (Ricchiuto and Bollerman, 2009).

$$\varepsilon_{wd} = \left(\frac{h_N}{L^{ref}}\right)^2$$

Other implementation details:

- **Dry cell identification:** use a wet/dry tolerance parameter ε_{wd} depending on grid characteristics (Ricchiuto and Bollerman, 2009).

$$\varepsilon_{wd} = \left(\frac{h_N}{L^{ref}}\right)^2$$

- **Boundary conditions:** use the theory of characteristics for: weak formulation for the NVFV scheme and ghost cells for CCFV scheme.

Other implementation details:

- **Dry cell identification:** use a wet/dry tolerance parameter ε_{wd} depending on grid characteristics (Ricchiuto and Bollerman, 2009).

$$\varepsilon_{wd} = \left(\frac{h_N}{L^{ref}}\right)^2$$

- **Boundary conditions:** use the theory of characteristics for: weak formulation for the NVFV scheme and ghost cells for CCFV scheme.

- Apply a four stage **2nd order Runge-Kutta scheme**, due to its enhanced stability region, under the CFL condition

$$\Delta t^n = CFL \cdot \min_i \left(\frac{R_i}{\left(\sqrt{u^2+v^2}+c\right)_i}\right).$$

Other implementation details:

- **Dry cell identification:** use a wet/dry tolerance parameter ε_{wd} depending on grid characteristics (Ricchiuto and Bollerman, 2009).

$$\varepsilon_{wd} = \left(\frac{h_N}{L^{ref}}\right)^2$$

- **Boundary conditions:** use the theory of characteristics for: weak formulation for the NVFV scheme and ghost cells for CCFV scheme.

- Apply a four stage **2nd order Runge-Kutta scheme**, due to its enhanced stability region, under the CFL condition

$$\Delta t^n = CFL \cdot \min_i \left(\frac{R_i}{\left(\sqrt{u^2+v^2}+c\right)_i} \right).$$

- Semi-implicit or implicit treatment for the **friction source** term within each cell following Brufau et al., 2004 and Serrano-Pacheco et al., 2009.

NUMERICAL RESULTS and COMPARISONS

Scheme	Description
NCFV	Node-Centered FV Scheme
CCFVc1	Cell-Centered FV compact (naive) reconstruction stencil
CCFVc2	Cell-Centered FV compact reconstruction stencil (corrected)
CCFVw1	Cell-Centered FV wide (naive) reconstruction stencil
CCFVw2	Cell-Centered FV wide reconstruction stencil (corrected)

NUMERICAL RESULTS and COMPARISONS

Scheme	Description
NCFV	Node-Centered FV Scheme
CCFVc1	Cell-Centered FV compact (naive) reconstruction stencil
CCFVc2	Cell-Centered FV compact reconstruction stencil (corrected)
CCFVw1	Cell-Centered FV wide (naive) reconstruction stencil
CCFVw2	Cell-Centered FV wide reconstruction stencil (corrected)

A traveling vortex solution (with periodic boundary conditions)

NUMERICAL RESULTS and COMPARISONS

Scheme	Description
NCFV	Node-Centered FV Scheme
CCFVc1	Cell-Centered FV compact (naive) reconstruction stencil
CCFVc2	Cell-Centered FV compact reconstruction stencil (corrected)
CCFVw1	Cell-Centered FV wide (naive) reconstruction stencil
CCFVw2	Cell-Centered FV wide reconstruction stencil (corrected)

A traveling vortex solution (with periodic boundary conditions)

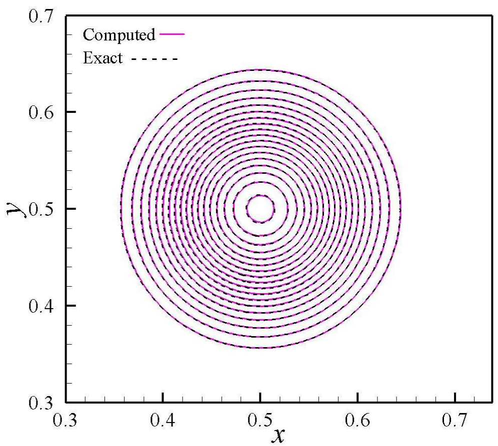

NUMERICAL RESULTS and COMPARISONS

Scheme	Description
NCFV	Node-Centered FV Scheme
CCFVc1	Cell-Centered FV compact (naive) reconstruction stencil
CCFVc2	Cell-Centered FV compact reconstruction stencil (corrected)
CCFVw1	Cell-Centered FV wide (naive) reconstruction stencil
CCFVw2	Cell-Centered FV wide reconstruction stencil (corrected)

A traveling vortex solution (with periodic boundary conditions)

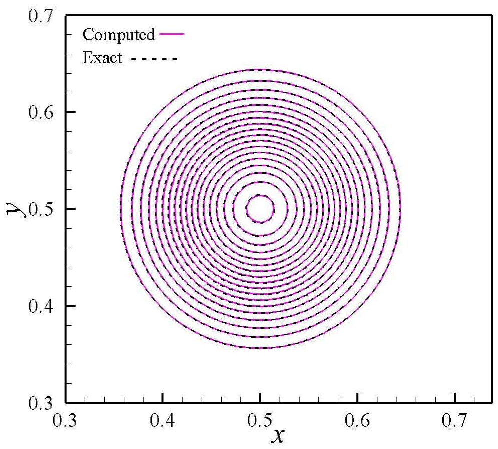

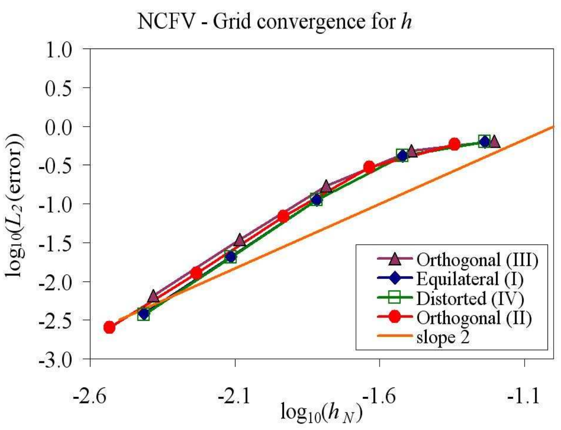

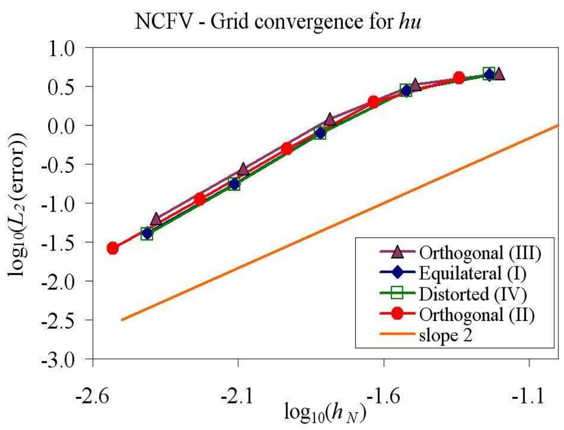

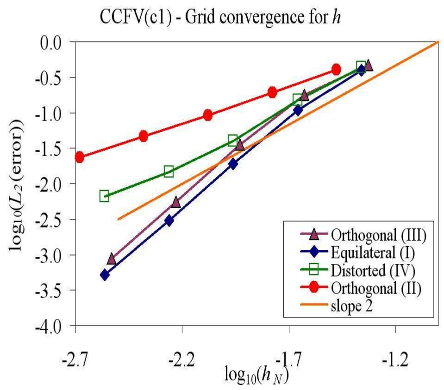
CCFV(c1) - Grid convergence for h
0.0
-0.5
-1.0
-1.5
-2.0
-2.5
-3.0
-3.5
-4.0
-2.7
-2.2
-1.7
-1.2
log10(L2(error))
log10(hN)
Orthogonal (III)
Equilateral (I)
Distorted (IV)
Orthogonal (II)
slope 2

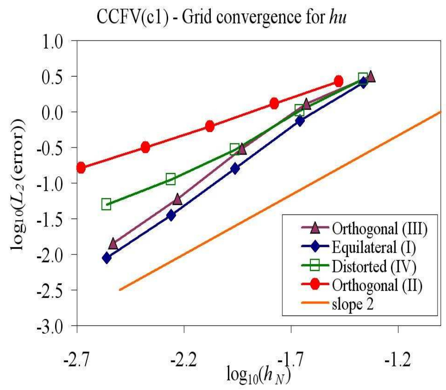
CCFV(c1) - Grid convergence for hu
1.0
0.5
0.0
-0.5
-1.0
-1.5
-2.0
-2.5
-3.0
-2.7
-2.2
-1.7
-1.2
log10(L2(error))
log10(hN)
Orthogonal (III)
Equilateral (I)
Distorted (IV)
Orthogonal (II)
slope 2

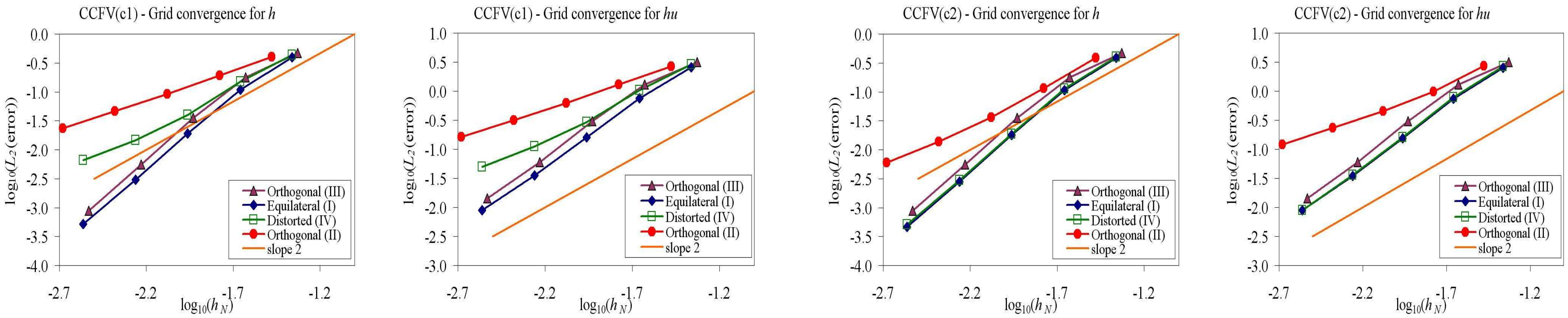
CCFV(c1) - Grid convergence for h
CCFV(c1) - Grid convergence for hu
CCFV(c2) - Grid convergence for h
CCFV(c2) - Grid convergence for hu
log10(L2(error))
log10(hN)
Orthogonal (III)
Equilateral (I)
Distorted (IV)
Orthogonal (II)
slope 2

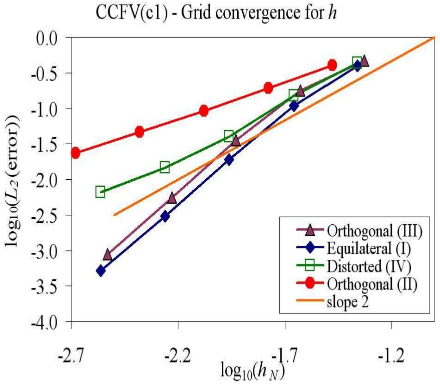
CCFV(c1) - Grid convergence for *h*
$\log_{10}(L_2(\text{error}))$
$\log_{10}(h_N)$
0.0
-0.5
-1.0
-1.5
-2.0
-2.5
-3.0
-3.5
-4.0
-2.7
-2.2
-1.7
-1.2
Orthogonal (III)
Equilateral (I)
Distorted (IV)
Orthogonal (II)
slope 2

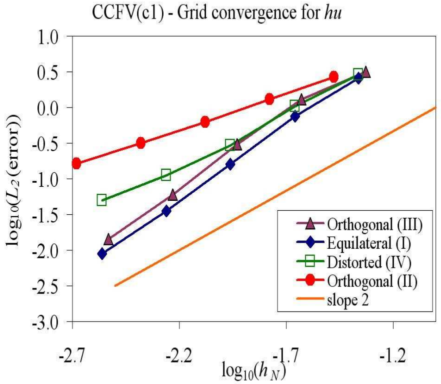
CCFV(c1) - Grid convergence for *hu*
$\log_{10}(L_2(\text{error}))$
$\log_{10}(h_N)$
1.0
0.5
0.0
-0.5
-1.0
-1.5
-2.0
-2.5
-3.0
-2.7
-2.2
-1.7
-1.2
Orthogonal (III)
Equilateral (I)
Distorted (IV)
Orthogonal (II)
slope 2

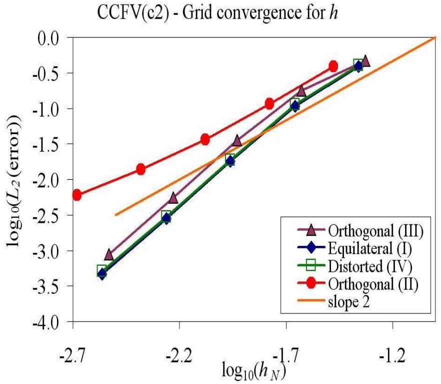
CCFV(c2) - Grid convergence for *h*
$\log_{10}(L_2(\text{error}))$
$\log_{10}(h_N)$
0.0
-0.5
-1.0
-1.5
-2.0
-2.5
-3.0
-3.5
-4.0
-2.7
-2.2
-1.7
-1.2
Orthogonal (III)
Equilateral (I)
Distorted (IV)
Orthogonal (II)
slope 2

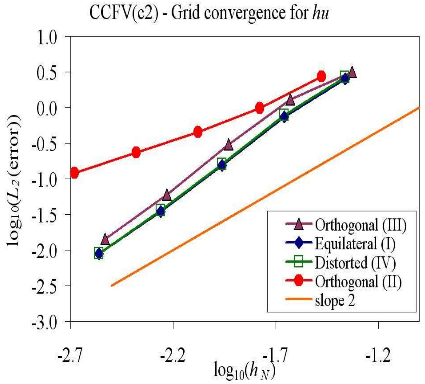
CCFV(c2) - Grid convergence for *hu*
$\log_{10}(L_2(\text{error}))$
$\log_{10}(h_N)$
1.0
0.5
0.0
-0.5
-1.0
-1.5
-2.0
-2.5
-3.0
-2.7
-2.2
-1.7
-1.2
Orthogonal (III)
Equilateral (I)
Distorted (IV)
Orthogonal (II)
slope 2

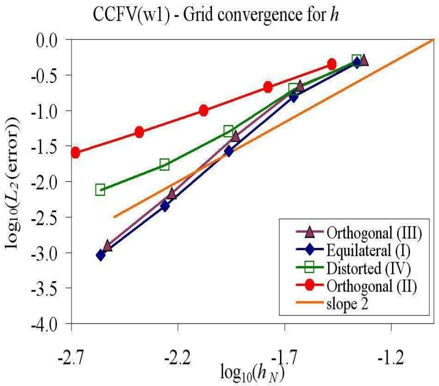
CCFV(w1) - Grid convergence for *h*
$\log_{10}(L_2(\text{error}))$
$\log_{10}(h_N)$
0.0
-0.5
-1.0
-1.5
-2.0
-2.5
-3.0
-3.5
-4.0
-2.7
-2.2
-1.7
-1.2
Orthogonal (III)
Equilateral (I)
Distorted (IV)
Orthogonal (II)
slope 2

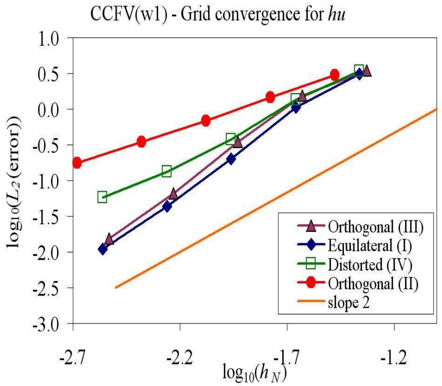
CCFV(w1) - Grid convergence for *hu*
$\log_{10}(L_2(\text{error}))$
$\log_{10}(h_N)$
1.0
0.5
0.0
-0.5
-1.0
-1.5
-2.0
-2.5
-3.0
-2.7
-2.2
-1.7
-1.2
Orthogonal (III)
Equilateral (I)
Distorted (IV)
Orthogonal (II)
slope 2

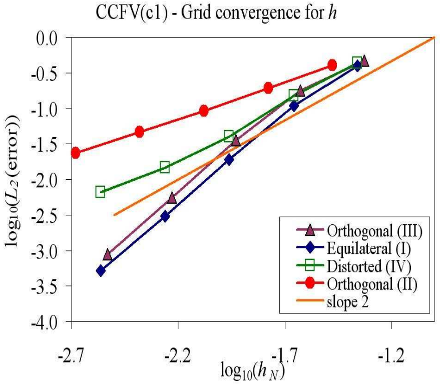
CCFV(c1) - Grid convergence for h
log10(L2(error))
log10(hN)
Orthogonal (III)
Equilateral (I)
Distorted (IV)
Orthogonal (II)
slope 2

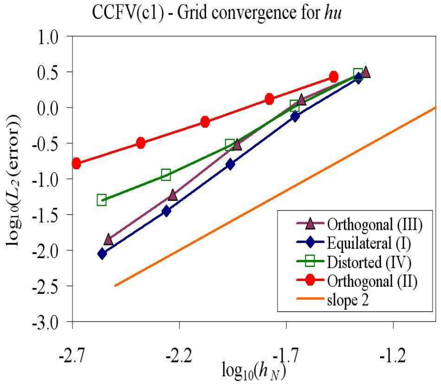
CCFV(c1) - Grid convergence for hu
log10(L2(error))
log10(hN)
Orthogonal (III)
Equilateral (I)
Distorted (IV)
Orthogonal (II)
slope 2

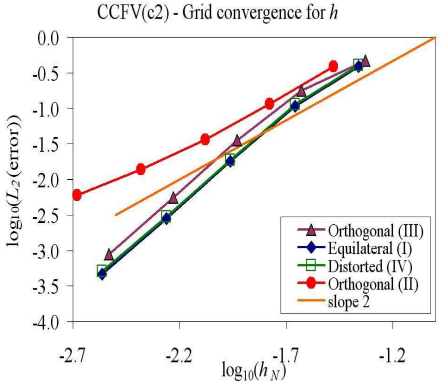
CCFV(c2) - Grid convergence for h
log10(L2(error))
log10(hN)
Orthogonal (III)
Equilateral (I)
Distorted (IV)
Orthogonal (II)
slope 2

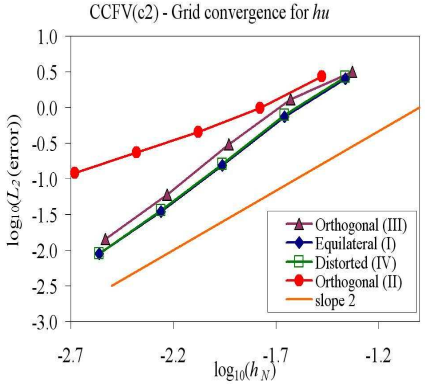
CCFV(c2) - Grid convergence for hu
log10(L2(error))
log10(hN)
Orthogonal (III)
Equilateral (I)
Distorted (IV)
Orthogonal (II)
slope 2

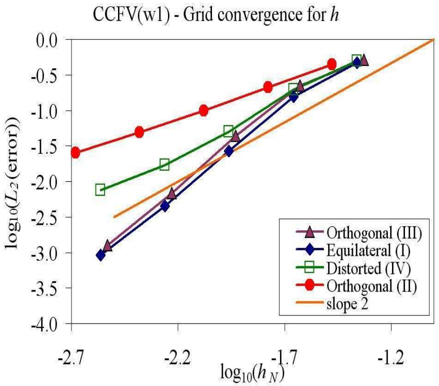
CCFV(w1) - Grid convergence for h
log10(L2(error))
log10(hN)
Orthogonal (III)
Equilateral (I)
Distorted (IV)
Orthogonal (II)
slope 2

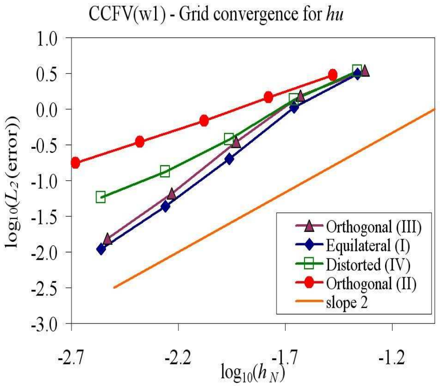
CCFV(w1) - Grid convergence for hu
log10(L2(error))
log10(hN)
Orthogonal (III)
Equilateral (I)
Distorted (IV)
Orthogonal (II)
slope 2

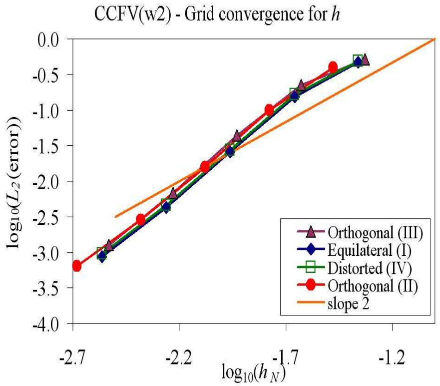
CCFV(w2) - Grid convergence for h
log10(L2(error))
log10(hN)
Orthogonal (III)
Equilateral (I)
Distorted (IV)
Orthogonal (II)
slope 2

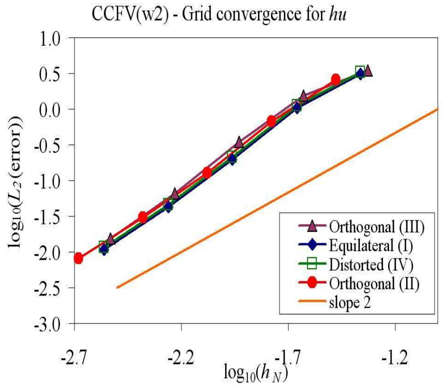
CCFV(w2) - Grid convergence for hu
log10(L2(error))
log10(hN)
Orthogonal (III)
Equilateral (I)
Distorted (IV)
Orthogonal (II)
slope 2

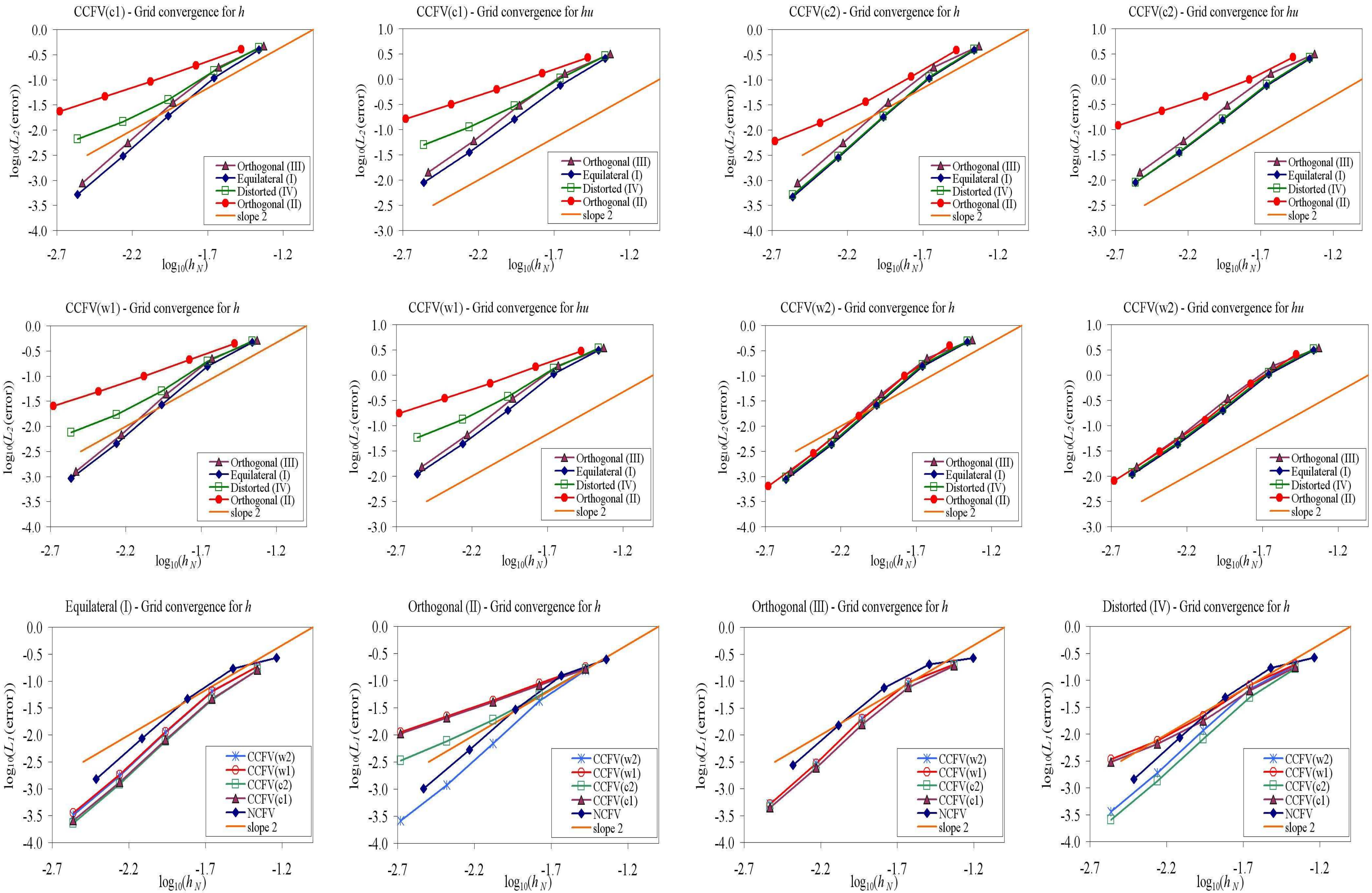

CCFV(c1) - Grid convergence for h
CCFV(c1) - Grid convergence for hu
CCFV(c2) - Grid convergence for h
CCFV(c2) - Grid convergence for hu
CCFV(w1) - Grid convergence for h
CCFV(w1) - Grid convergence for hu
CCFV(w2) - Grid convergence for h
CCFV(w2) - Grid convergence for hu
Equilateral (I) - Grid convergence for h
Orthogonal (II) - Grid convergence for h
Orthogonal (III) - Grid convergence for h
Distorted (IV) - Grid convergence for h
log10(L2(error))
log10(L1(error))
log10(hN)
Orthogonal (III)
Equilateral (I)
Distorted (IV)
Orthogonal (II)
slope 2
CCFV(w2)
CCFV(w1)
CCFV(c2)
CCFV(c1)
NCFV

A 2D potential (steady) solution with topography

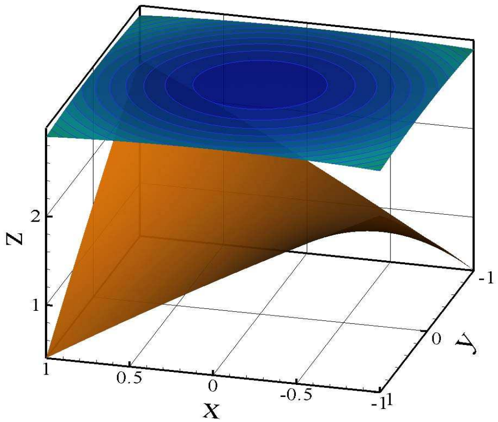

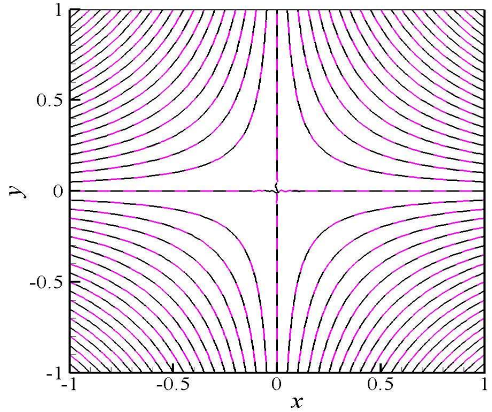

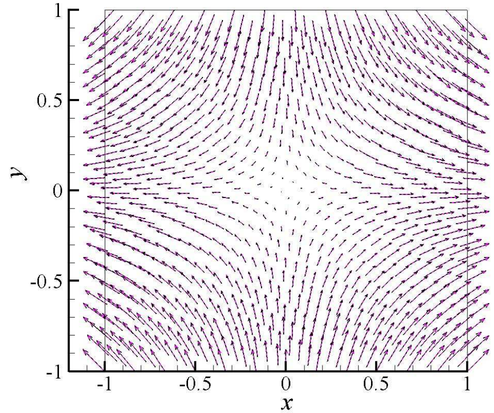

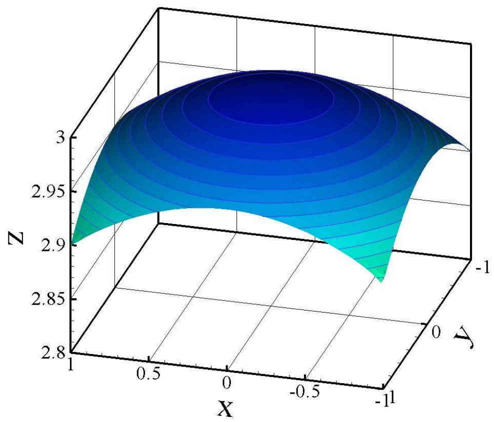

A 2D potential (steady) solution with topography

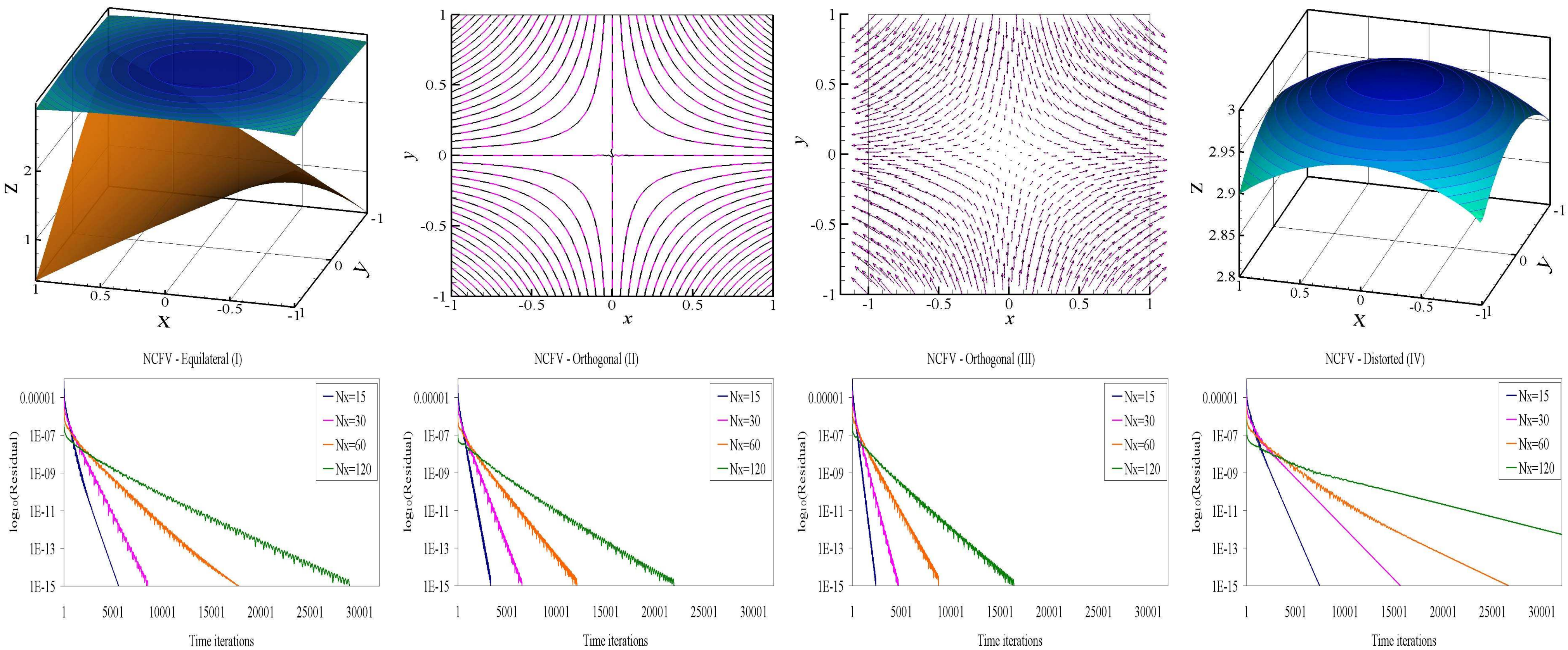

A 2D potential (steady) solution with topography

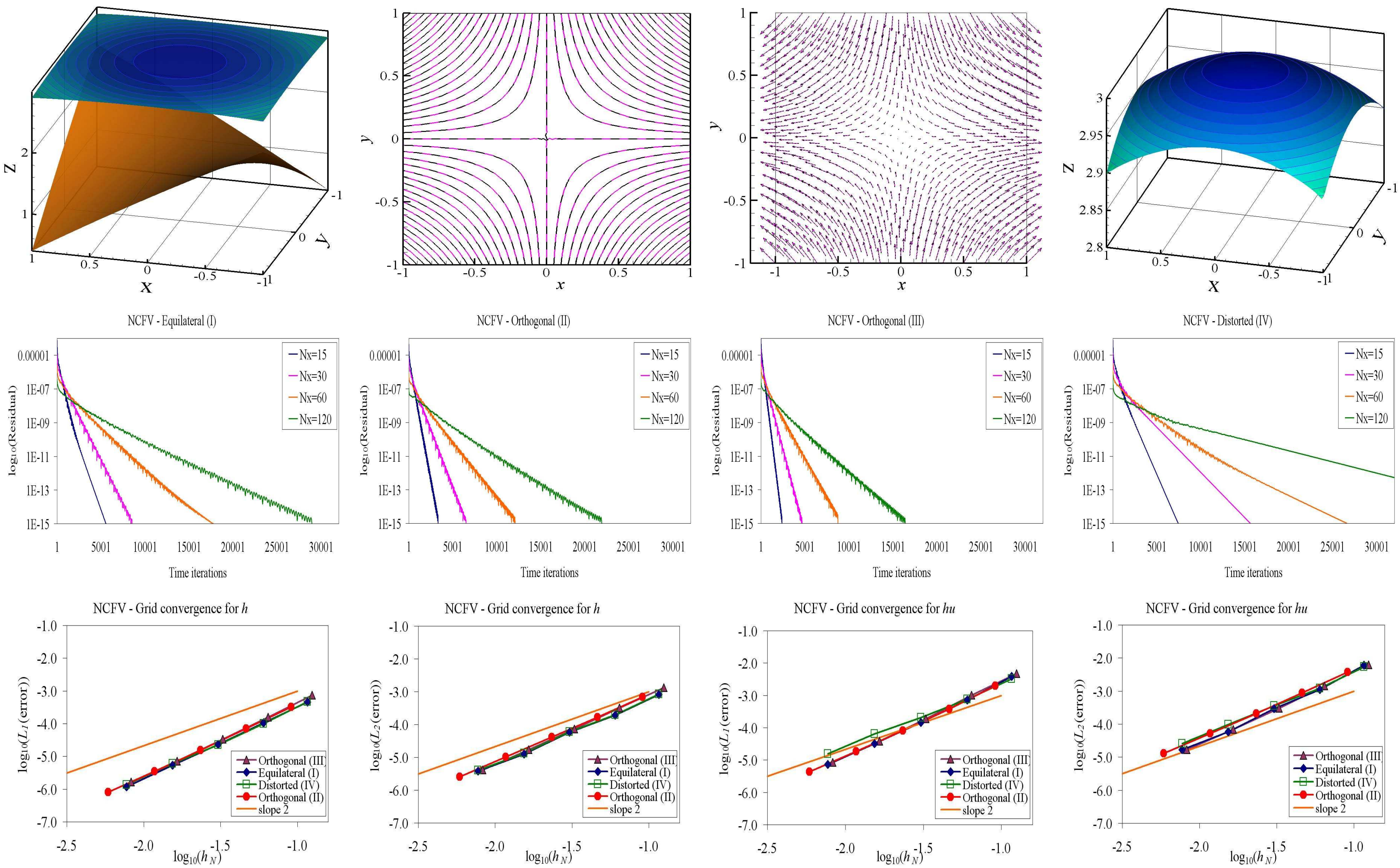

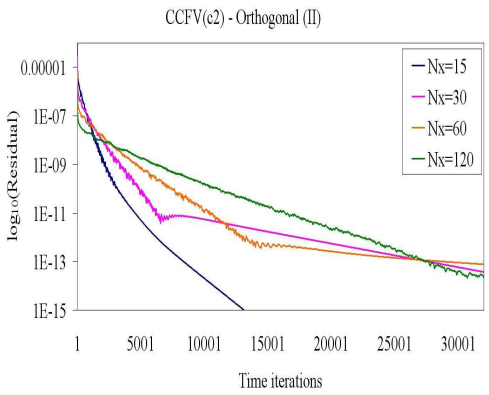
CCFV(c2) - Orthogonal (II)
log10(Residual)
Time iterations
Nx=15
Nx=30
Nx=60
Nx=120

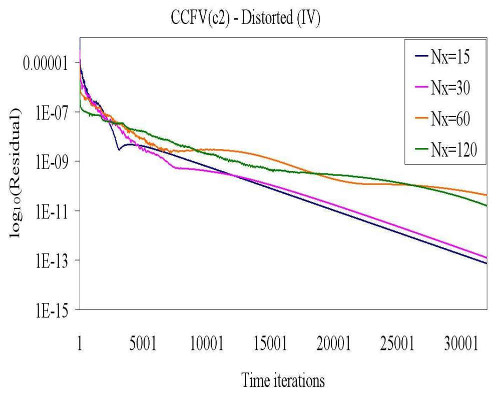
CCFV(c2) - Distorted (IV)
log10(Residual)
Time iterations
Nx=15
Nx=30
Nx=60
Nx=120

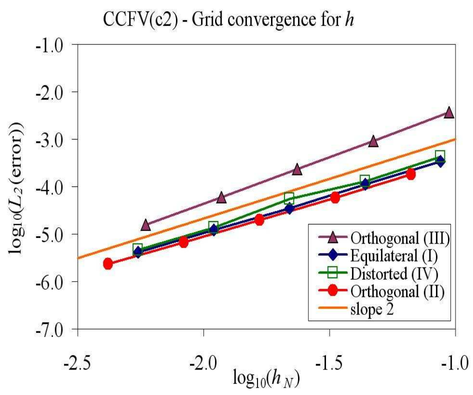
CCFV(c2) - Grid convergence for h
log10(L2(error))
log10(h N)
Orthogonal (III)
Equilateral (I)
Distorted (IV)
Orthogonal (II)
slope 2

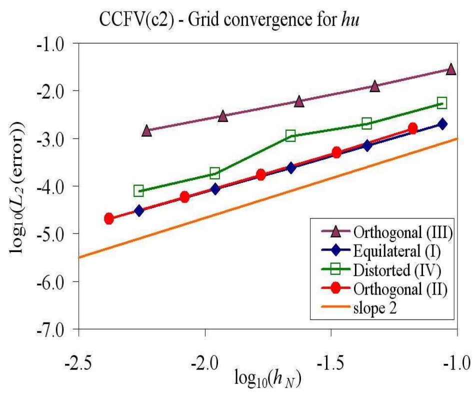
CCFV(c2) - Grid convergence for hu
log10(L2(error))
log10(h N)
Orthogonal (III)
Equilateral (I)
Distorted (IV)
Orthogonal (II)
slope 2

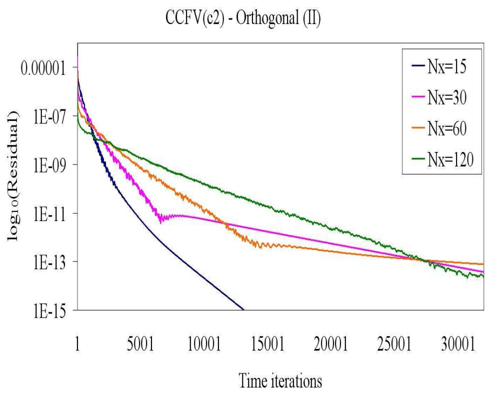
CCFV(c2) - Orthogonal (II)
log₁₀(Residual)
Time iterations
Nx=15
Nx=30
Nx=60
Nx=120

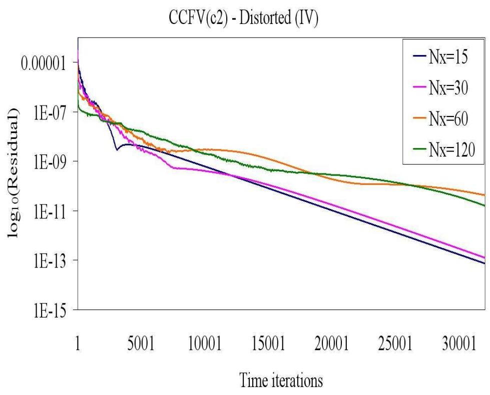
CCFV(c2) - Distorted (IV)
log₁₀(Residual)
Time iterations
Nx=15
Nx=30
Nx=60
Nx=120

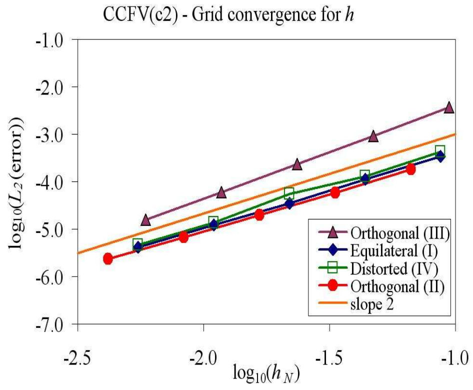
CCFV(c2) - Grid convergence for h
log10(L2(error))
log10(hN)
Orthogonal (III)
Equilateral (I)
Distorted (IV)
Orthogonal (II)
slope 2

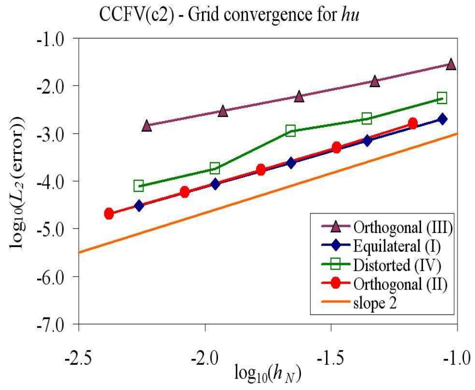
CCFV(c2) - Grid convergence for hu
log10(L2(error))
log10(hN)
Orthogonal (III)
Equilateral (I)
Distorted (IV)
Orthogonal (II)
slope 2

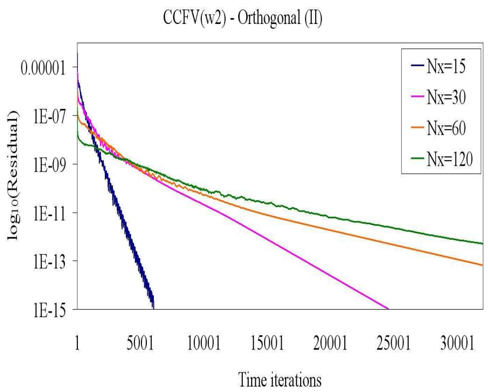
CCFV(w2) - Orthogonal (II)
log₁₀(Residual)
Time iterations
Nx=15
Nx=30
Nx=60
Nx=120

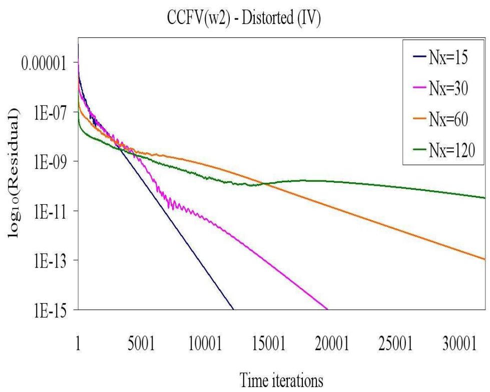
CCFV(w2) - Distorted (IV)
log₁₀(Residual)
Time iterations
Nx=15
Nx=30
Nx=60
Nx=120

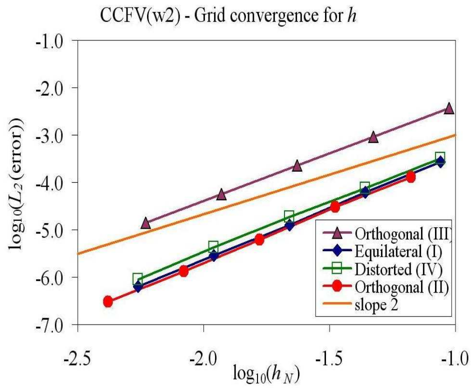
CCFV(w2) - Grid convergence for h
log10(L2(error))
log10(hN)
Orthogonal (III)
Equilateral (I)
Distorted (IV)
Orthogonal (II)
slope 2

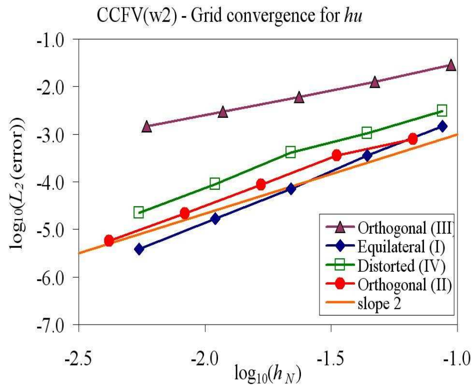
CCFV(w2) - Grid convergence for hu
log10(L2(error))
log10(hN)
Orthogonal (III)
Equilateral (I)
Distorted (IV)
Orthogonal (II)
slope 2

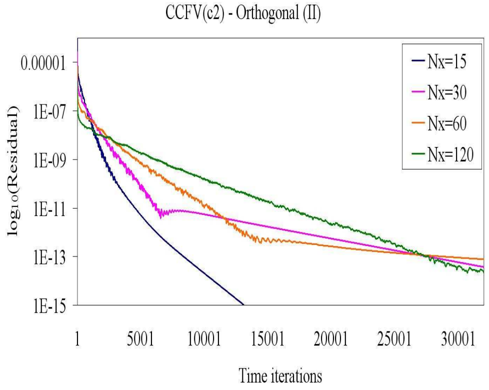
CCFV(c2) - Orthogonal (II)
log₁₀(Residual)
Nx=15
Nx=30
Nx=60
Nx=120
Time iterations

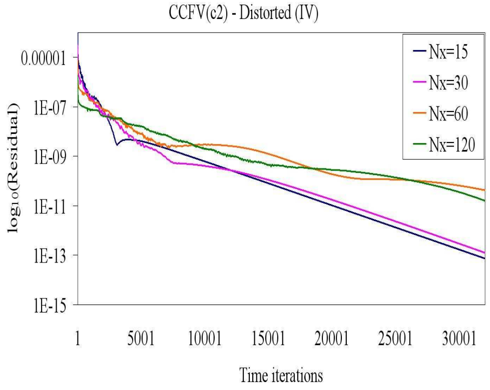
CCFV(c2) - Distorted (IV)
log₁₀(Residual)
Nx=15
Nx=30
Nx=60
Nx=120
Time iterations

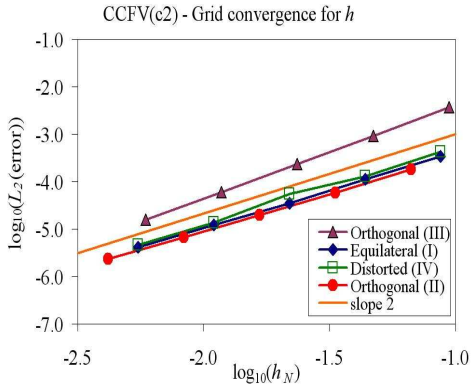
CCFV(c2) - Grid convergence for h
log10(L2(error))
Orthogonal (III)
Equilateral (I)
Distorted (IV)
Orthogonal (II)
slope 2
log10(hN)

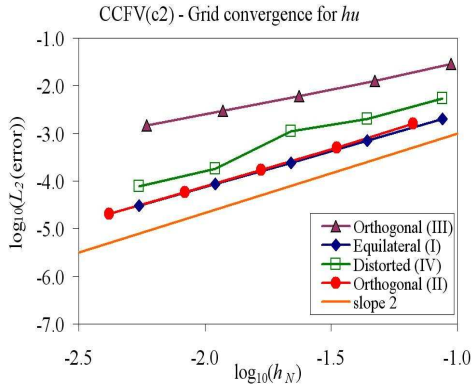
CCFV(c2) - Grid convergence for hu
log10(L2(error))
Orthogonal (III)
Equilateral (I)
Distorted (IV)
Orthogonal (II)
slope 2
log10(hN)

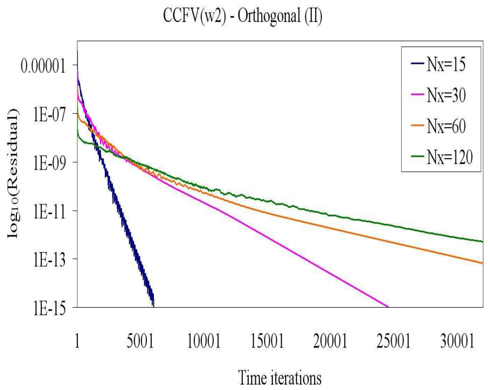
CCFV(w2) - Orthogonal (II)
log₁₀(Residual)
Nx=15
Nx=30
Nx=60
Nx=120
Time iterations

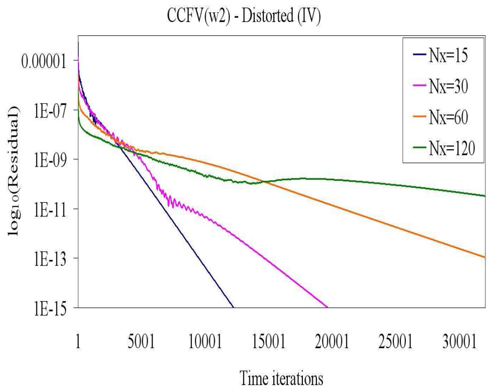
CCFV(w2) - Distorted (IV)
log₁₀(Residual)
Nx=15
Nx=30
Nx=60
Nx=120
Time iterations

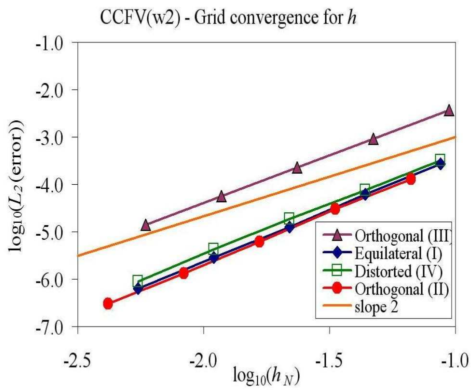
CCFV(w2) - Grid convergence for h
log10(L2(error))
Orthogonal (III)
Equilateral (I)
Distorted (IV)
Orthogonal (II)
slope 2
log10(hN)

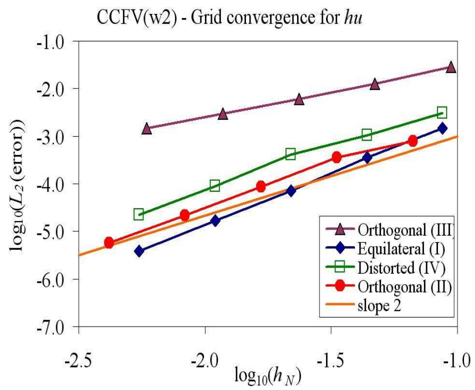
CCFV(w2) - Grid convergence for hu
log10(L2(error))
Orthogonal (III)
Equilateral (I)
Distorted (IV)
Orthogonal (II)
slope 2
log10(hN)

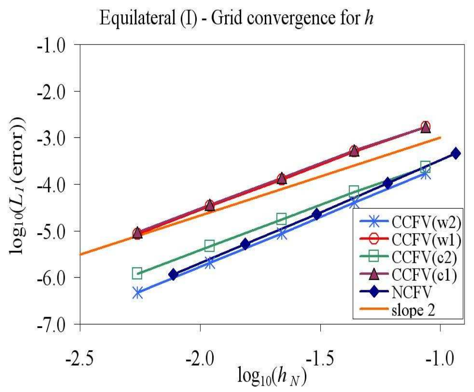
Equilateral (I) - Grid convergence for h
log10(L1(error))
CCFV(w2)
CCFV(w1)
CCFV(c2)
CCFV(c1)
NCFV
slope 2
log10(hN)

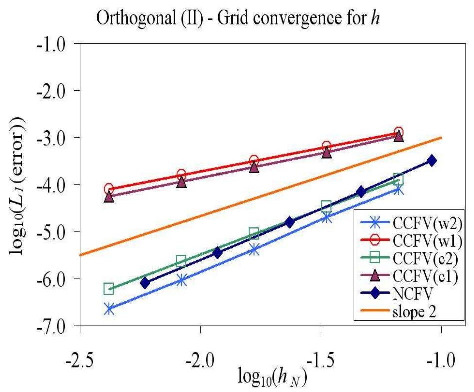
Orthogonal (II) - Grid convergence for h
log10(L1(error))
CCFV(w2)
CCFV(w1)
CCFV(c2)
CCFV(c1)
NCFV
slope 2
log10(hN)

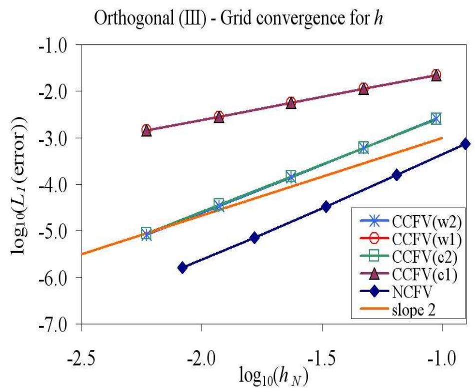
Orthogonal (III) - Grid convergence for h
log10(L1(error))
CCFV(w2)
CCFV(w1)
CCFV(c2)
CCFV(c1)
NCFV
slope 2
log10(hN)

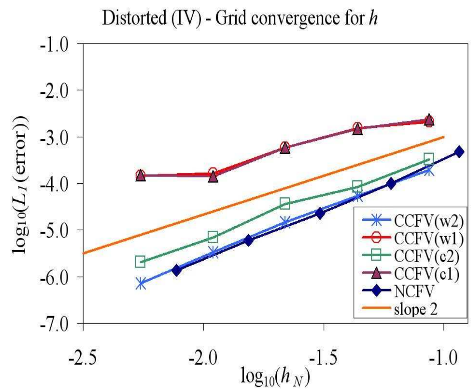
Distorted (IV) - Grid convergence for h
log10(L1(error))
CCFV(w2)
CCFV(w1)
CCFV(c2)
CCFV(c1)
NCFV
slope 2
log10(hN)

Grid convergence including dry boundaries: Thacker's 2D solutions

- Known analytical periodic solutions.
- The motion is oscillatory.
- Friction is not included.
- Difficult test (wetting and drying)
- Used it to check convergence rates.

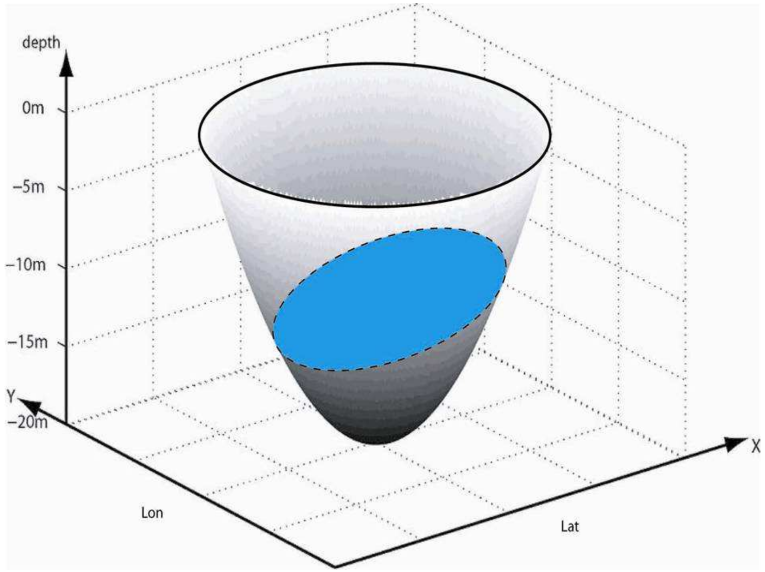

Grid convergence including dry boundaries: Thacker's 2D solutions

- Known analytical periodic solutions.
- The motion is oscillatory.
- Friction is not included.
- Difficult test (wetting and drying)
- Used it to check convergence rates.

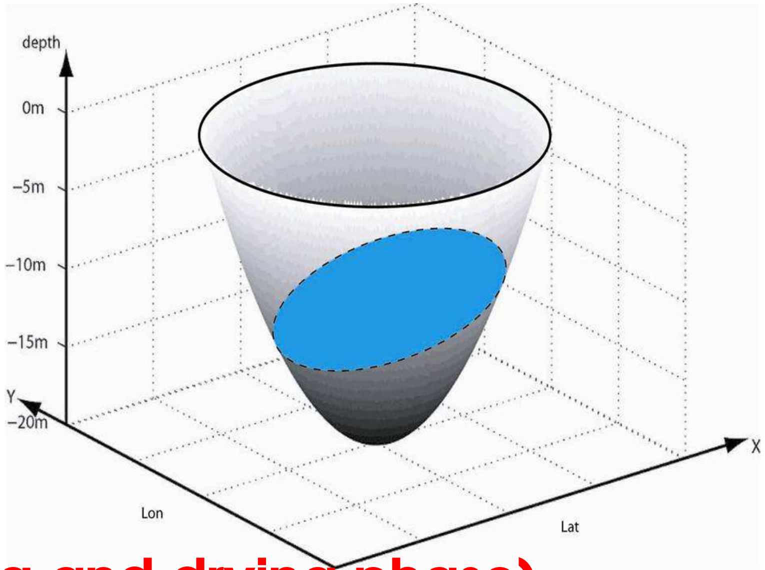

Thacker's axisymmetric solution (wetting and drying phase)

Grid convergence including dry boundaries: Thacker's 2D solutions

- Known analytical periodic solutions.
- The motion is oscillatory.
- Friction is not included.
- Difficult test (wetting and drying)
- Used it to check convergence rates.

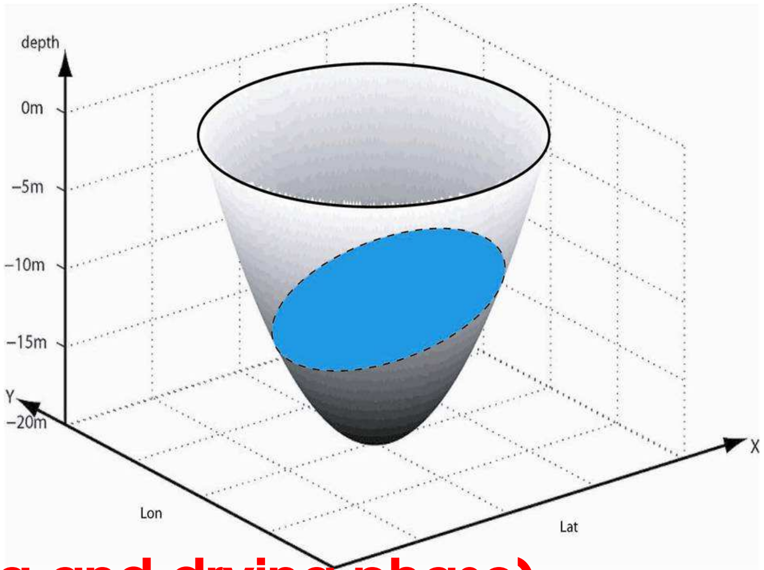

Thacker's axisymmetric solution (wetting and drying phase)

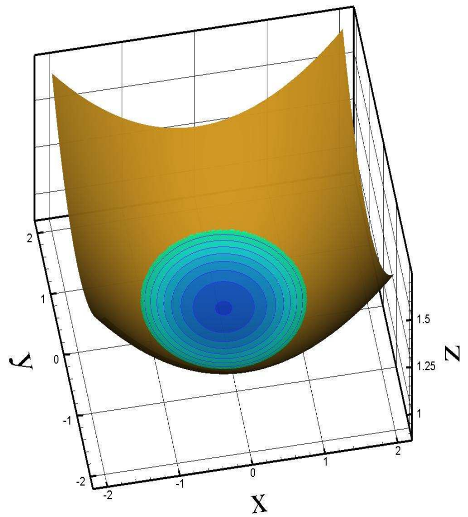

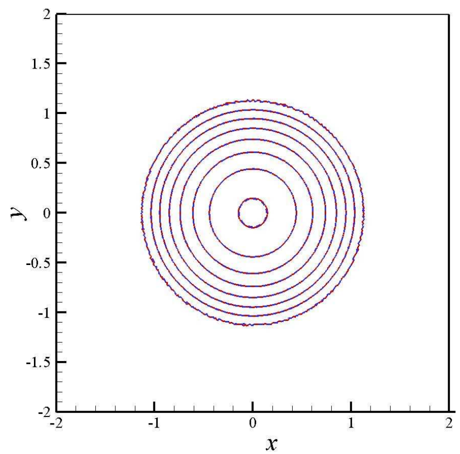

Grid convergence including dry boundaries: Thacker's 2D solutions

- Known analytical periodic solutions.
- The motion is oscillatory.
- Friction is not included.
- Difficult test (wetting and drying)
- Used it to check convergence rates.

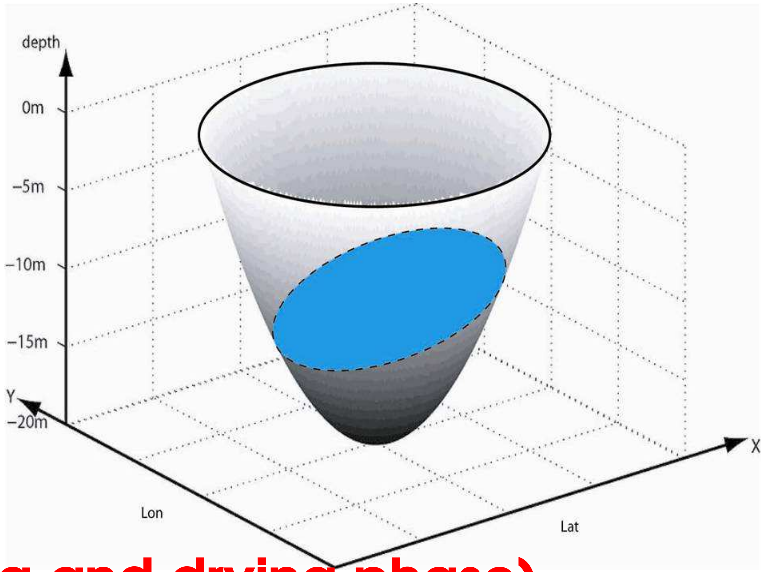

Thacker's axisymmetric solution (wetting and drying phase)

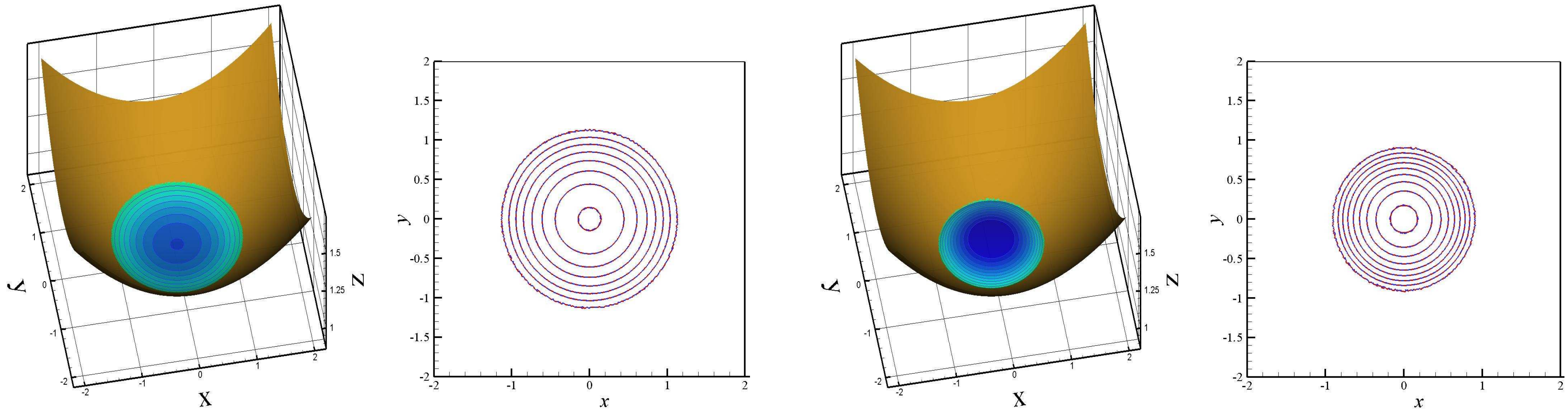

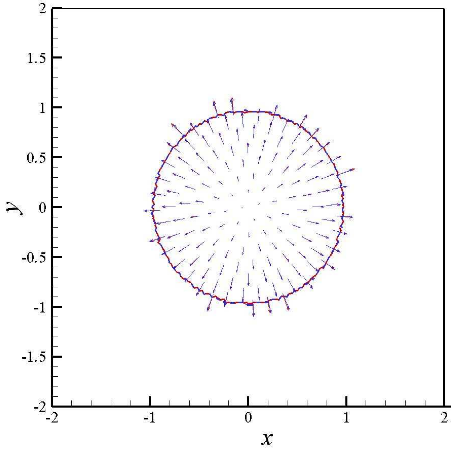

x
y

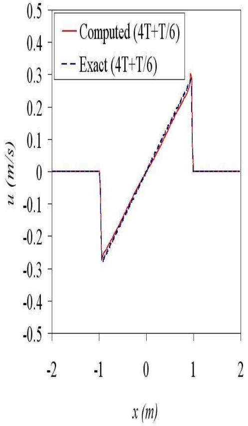

Computed (4T+T/6)
Exact (4T+T/6)
u (m/s)
x (m)

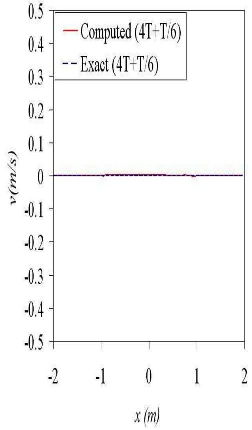

Computed (4T+T/6)
Exact (4T+T/6)
v(m/s)
x (m)

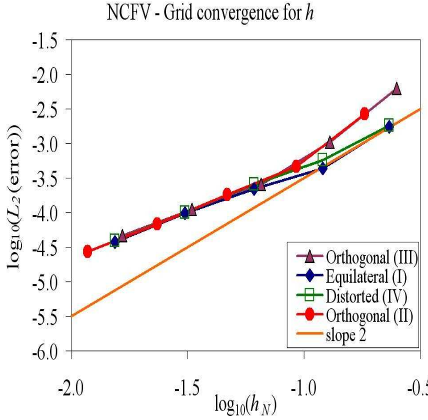

NCFV - Grid convergence for h
Orthogonal (III)
Equilateral (I)
Distorted (IV)
Orthogonal (II)
slope 2
log10(L2(error))
log10(hN)

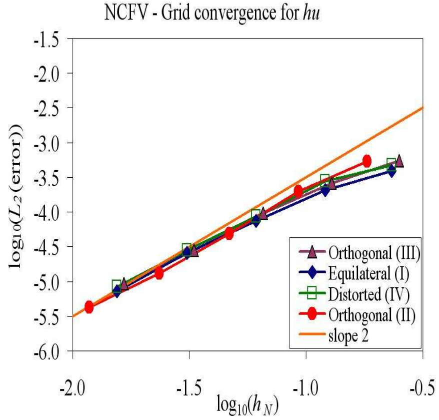

NCFV - Grid convergence for hu
Orthogonal (III)
Equilateral (I)
Distorted (IV)
Orthogonal (II)
slope 2
log10(L2(error))
log10(hN)

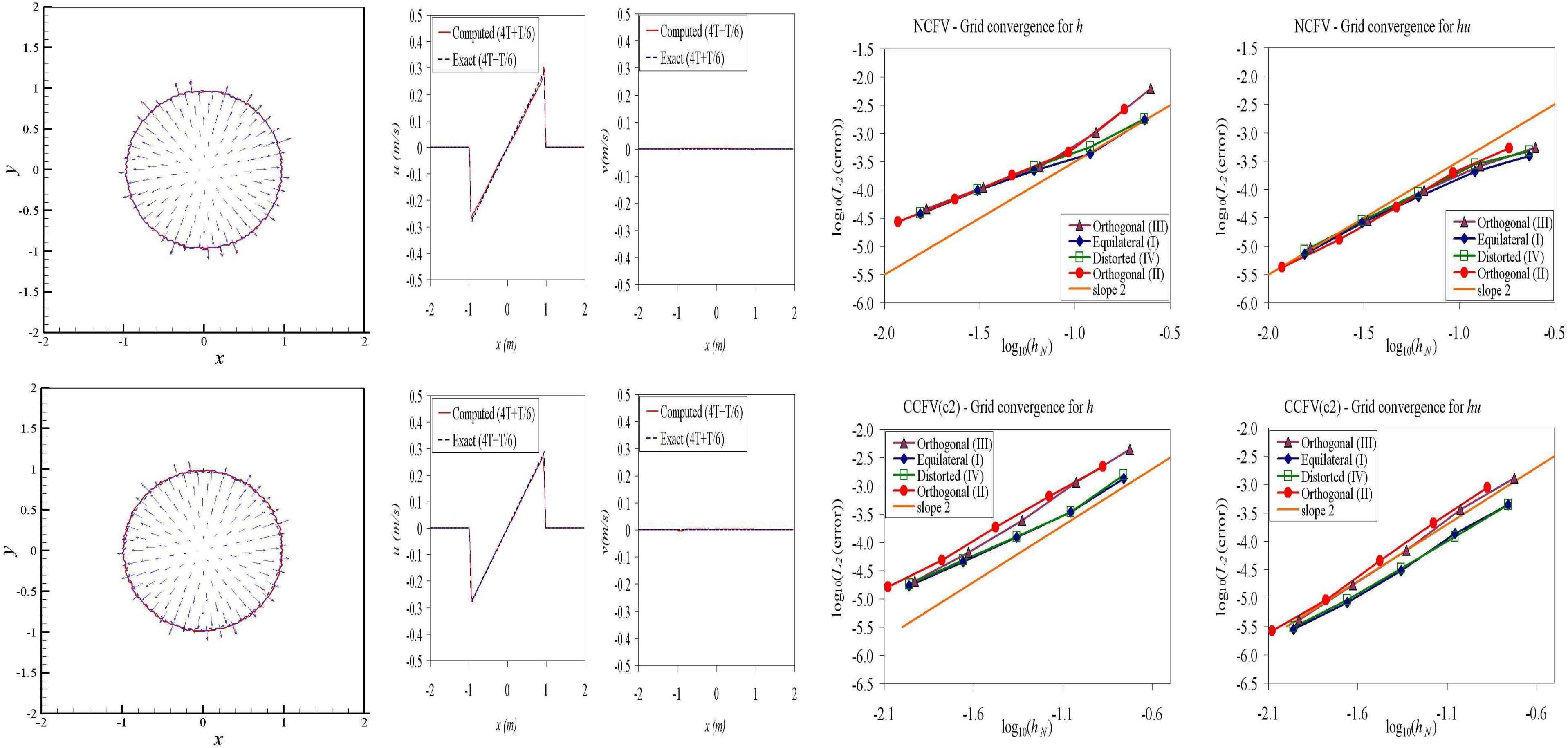

Computed (4T+T/6)
Exact (4T+T/6)
u (m/s)
v (m/s)
x (m)
x
y
NCFV - Grid convergence for h
NCFV - Grid convergence for hu
CCFV(c2) - Grid convergence for h
CCFV(c2) - Grid convergence for hu
log10(L2 (error))
log10(hN)
Orthogonal (III)
Equilateral (I)
Distorted (IV)
Orthogonal (II)
slope 2

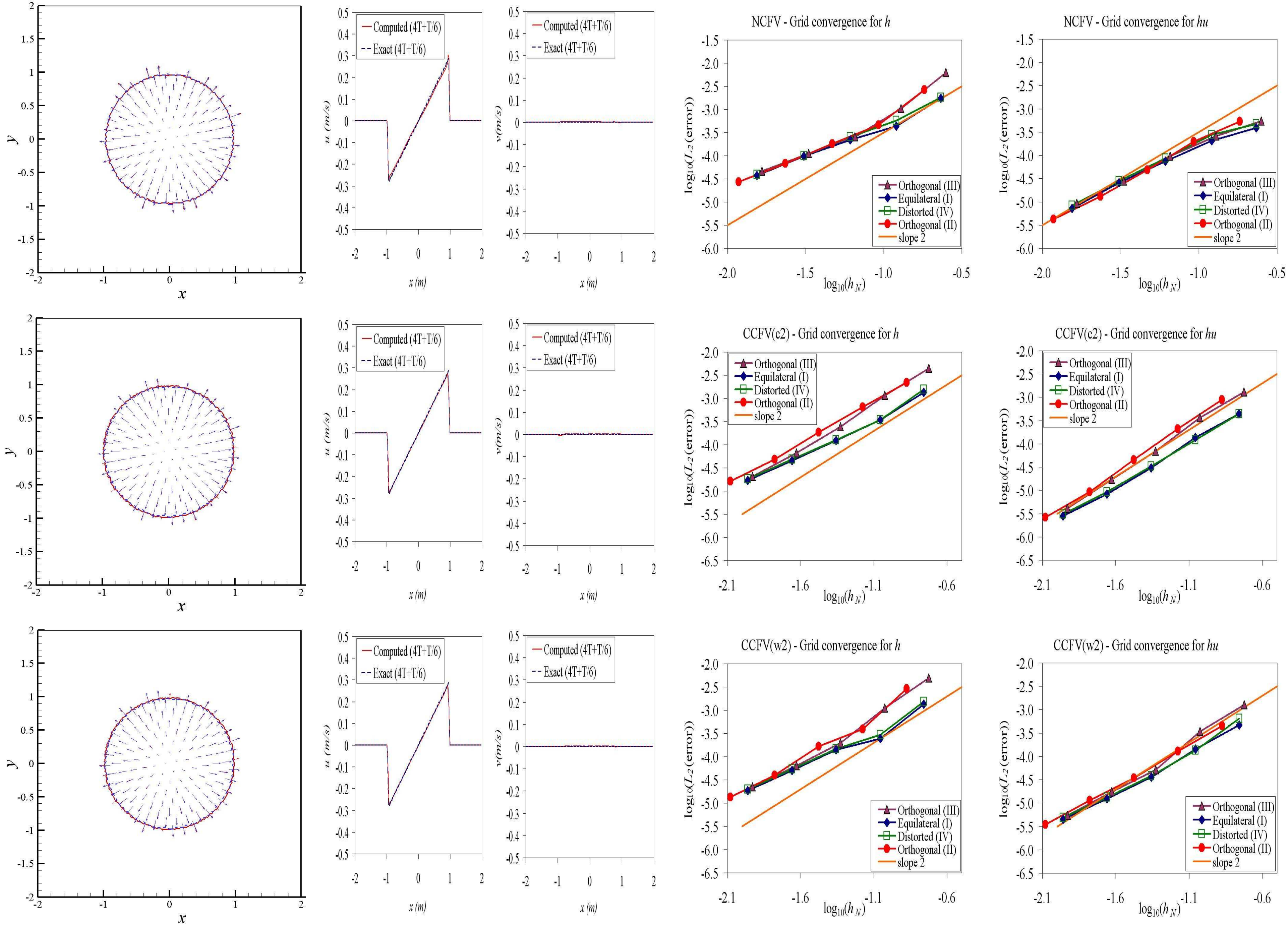

NCFV - Grid convergence for h
NCFV - Grid convergence for hu
CCFV(c2) - Grid convergence for h
CCFV(c2) - Grid convergence for hu
CCFV(w2) - Grid convergence for h
CCFV(w2) - Grid convergence for hu
Computed (4T+T/6)
Exact (4T+T/6)
Orthogonal (III)
Equilateral (I)
Distorted (IV)
Orthogonal (II)
slope 2
x
y
x (m)
u (m/s)
v (m/s)
log10(L2(error))
log10(hN)

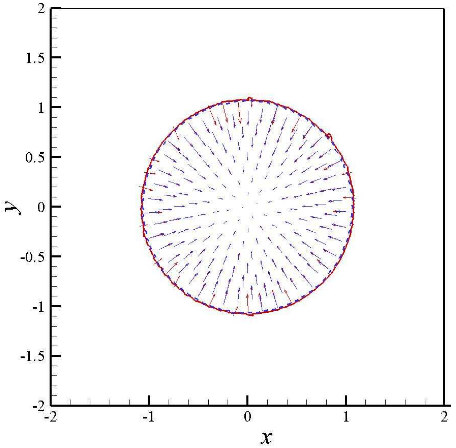

x
y

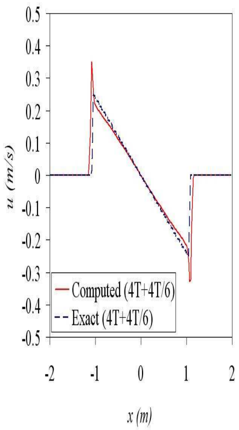

u (m/s)
x (m)
Computed (4T+4T/6)
Exact (4T+4T/6)

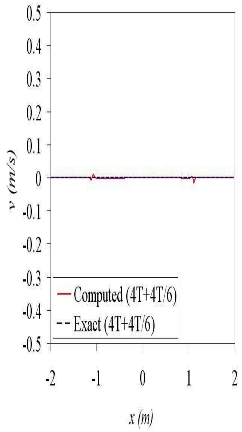

v (m/s)
x (m)
Computed (4T+4T/6)
Exact (4T+4T/6)

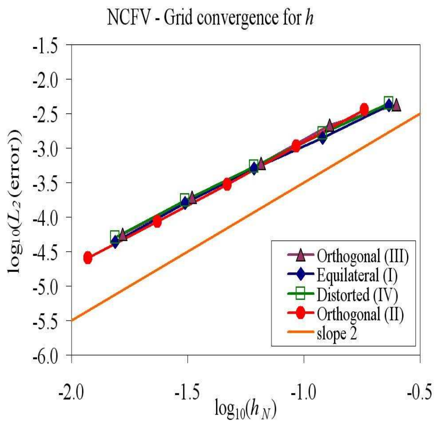

NCFV - Grid convergence for h
log10(L2(error))
log10(hN)
Orthogonal (III)
Equilateral (I)
Distorted (IV)
Orthogonal (II)
slope 2

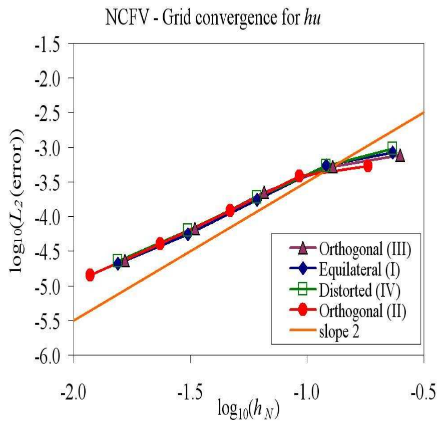

NCFV - Grid convergence for hu
log10(L2(error))
log10(hN)
Orthogonal (III)
Equilateral (I)
Distorted (IV)
Orthogonal (II)
slope 2

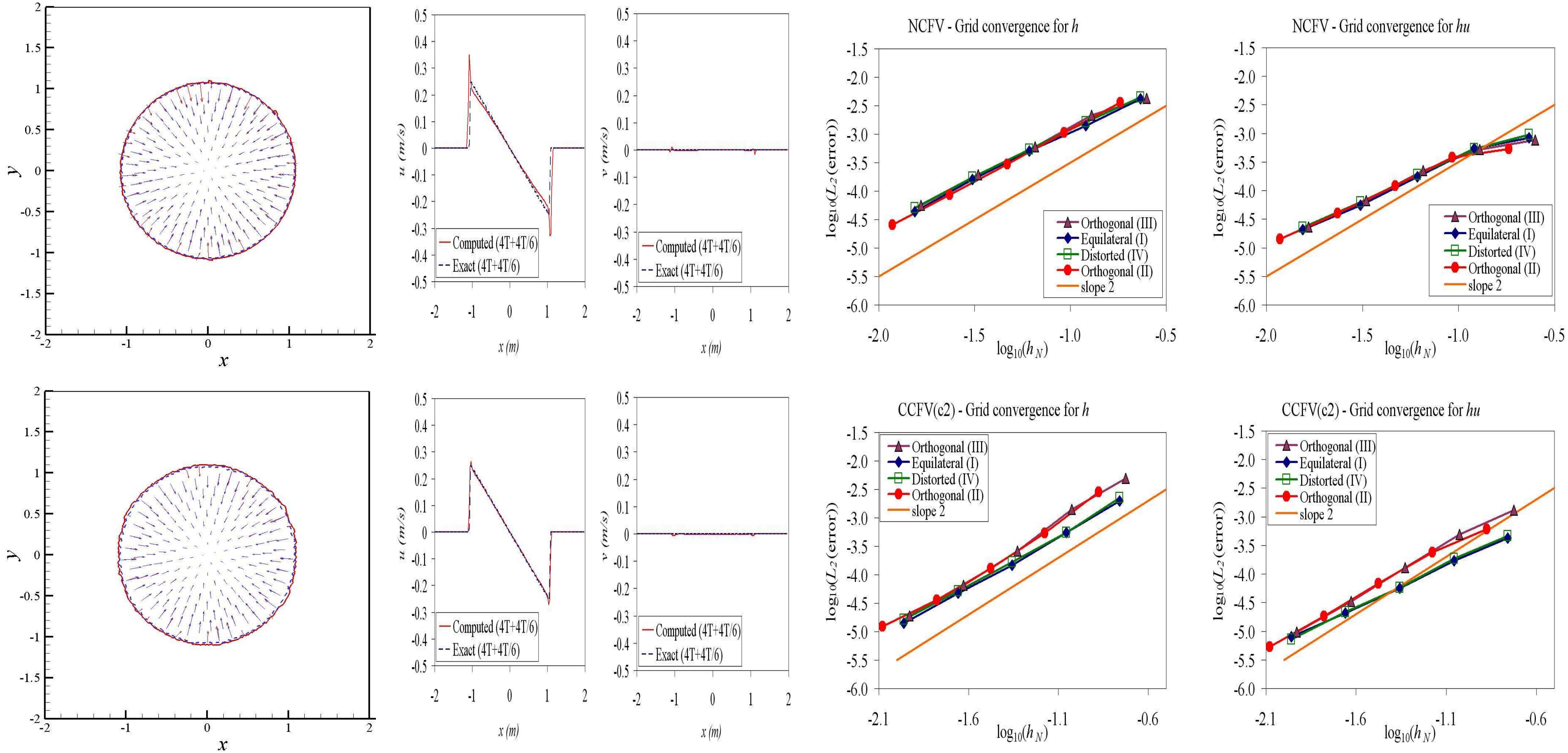

Computed (4T+4T/6)
Exact (4T+4T/6)
u (m/s)
v (m/s)
x (m)
x
y
NCFV - Grid convergence for h
NCFV - Grid convergence for hu
CCFV(c2) - Grid convergence for h
CCFV(c2) - Grid convergence for hu
Orthogonal (III)
Equilateral (I)
Distorted (IV)
Orthogonal (II)
slope 2
log10(L2(error))
log10(hN)

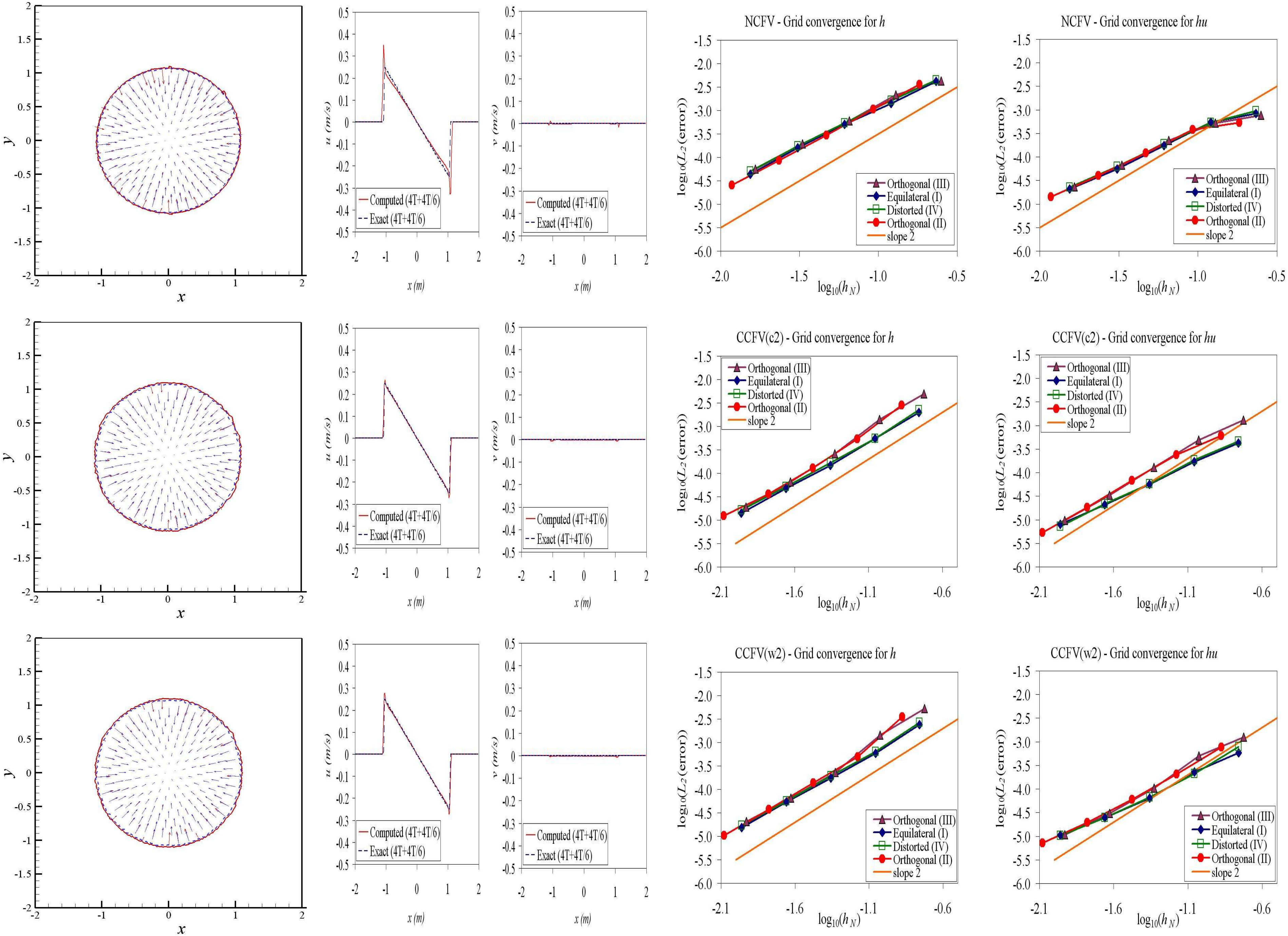
NCFV - Grid convergence for h
NCFV - Grid convergence for hu
CCFV(c2) - Grid convergence for h
CCFV(c2) - Grid convergence for hu
CCFV(w2) - Grid convergence for h
CCFV(w2) - Grid convergence for hu
Orthogonal (III)
Equilateral (I)
Distorted (IV)
Orthogonal (II)
slope 2
log10(L2(error))
log10(hN)
Computed (4T+4T/6)
Exact (4T+4T/6)
u (m/s)
v (m/s)
x (m)
x
y

The Maplasset dam-break test case (EDF grid, CFL=0.9, $n_m = 0.033$)

The Maplasset dam-break test case (EDF grid, CFL=0.9, $n_m = 0.033$)

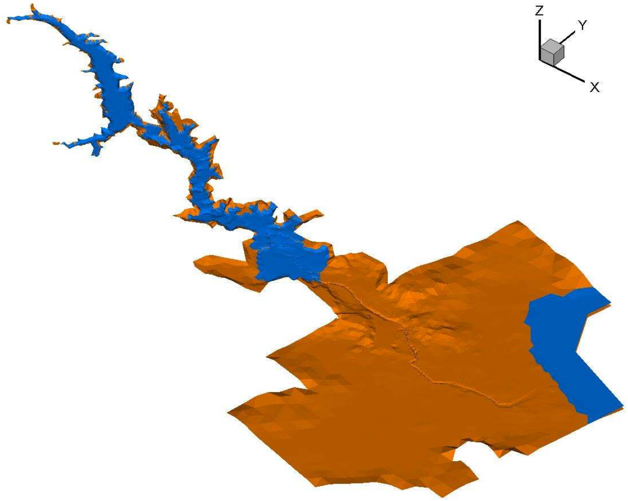

The Maplasset dam-break test case (EDF grid, CFL=0.9, $n_m = 0.033$)

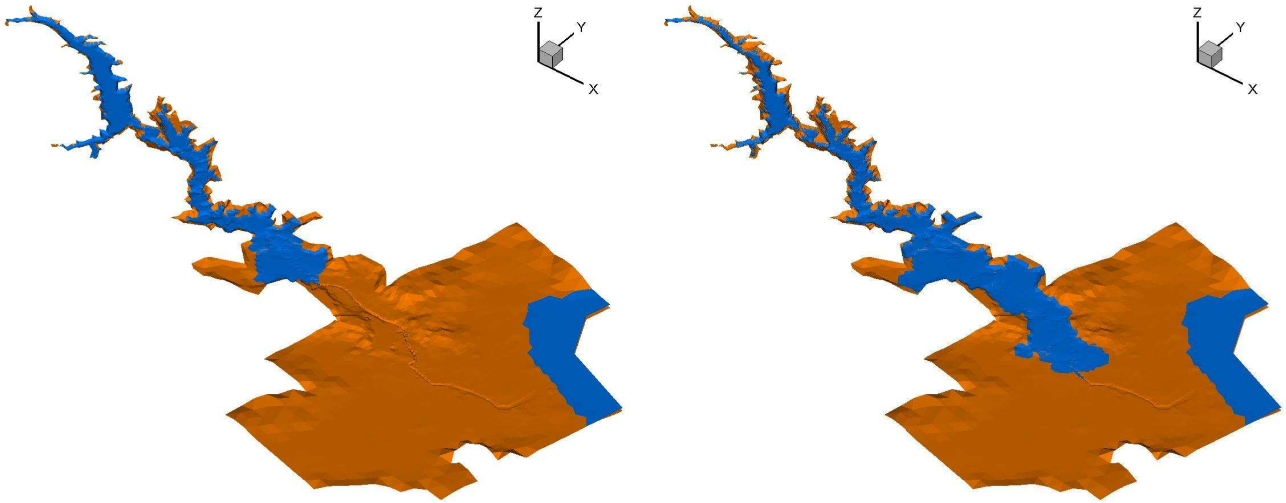

The Maplasset dam-break test case (EDF grid, CFL=0.9, $n_m = 0.033$)

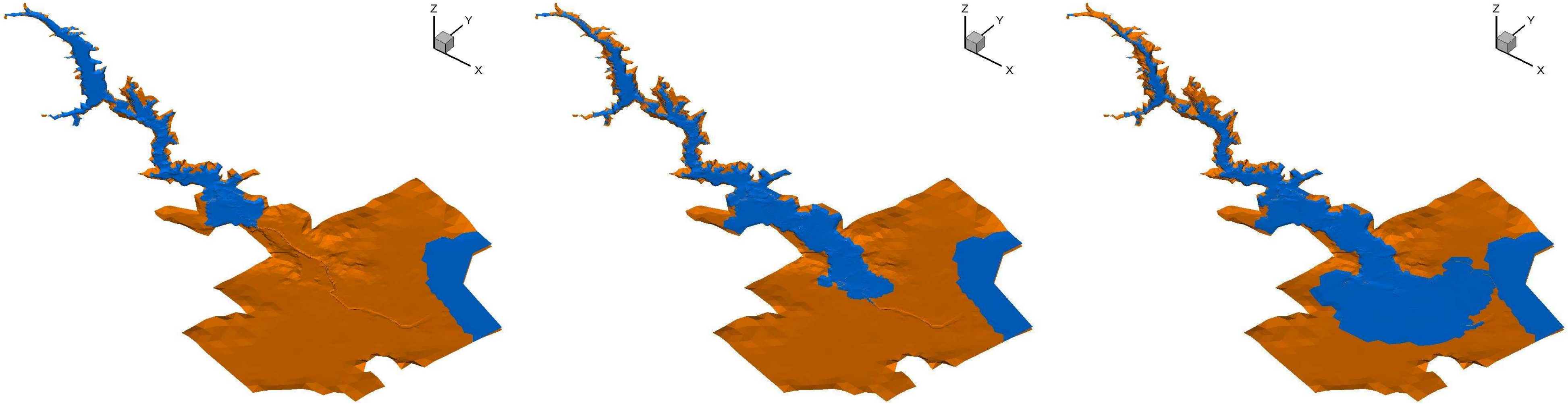

Water depth evolution at t=800s, 1600s, 2400s

The Maplasset dam-break test case (EDF grid, CFL=0.9, $n_m = 0.033$)

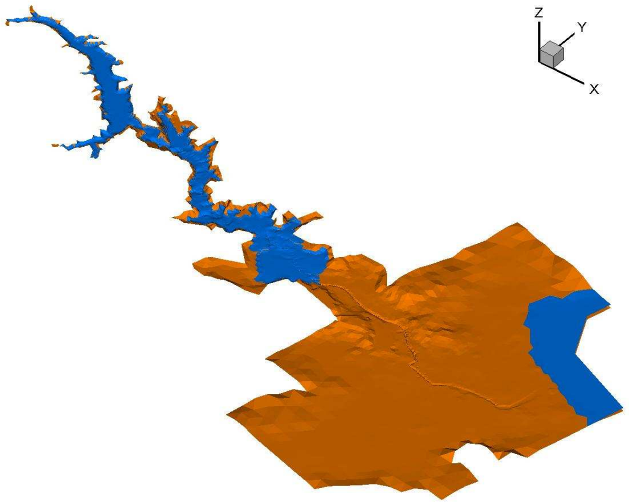

Water depth evolution at t=800s, 1600s, 2400s

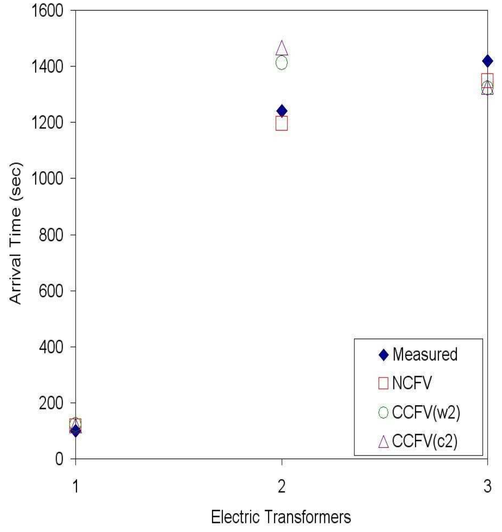

The Maplasset dam-break test case (EDF grid, CFL=0.9, $n_m = 0.033$)

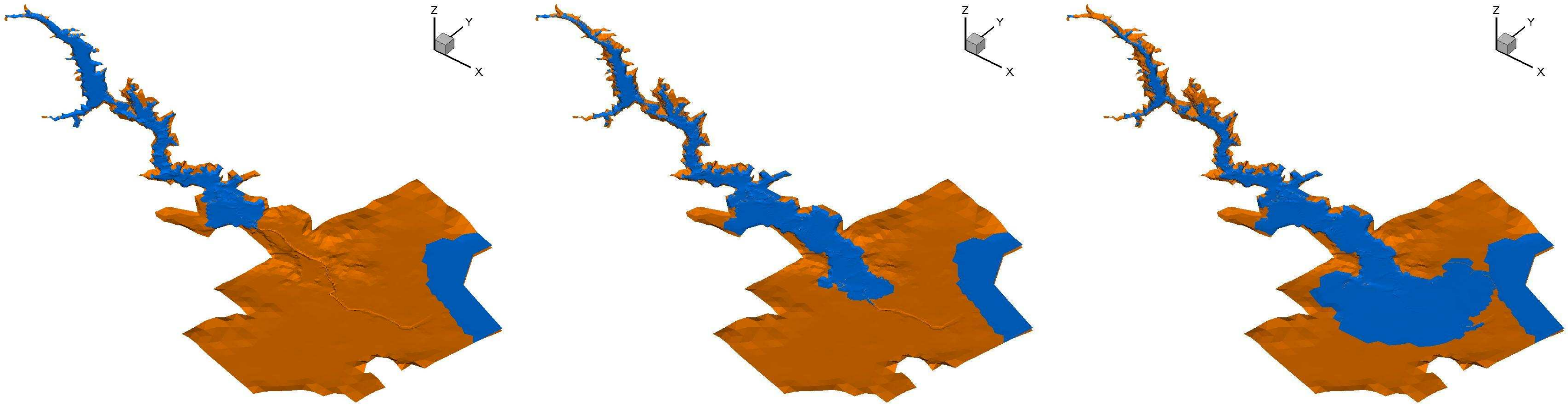

Water depth evolution at t=800s, 1600s, 2400s

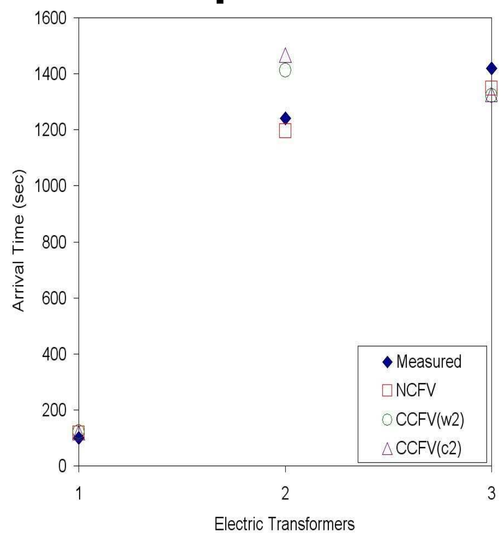

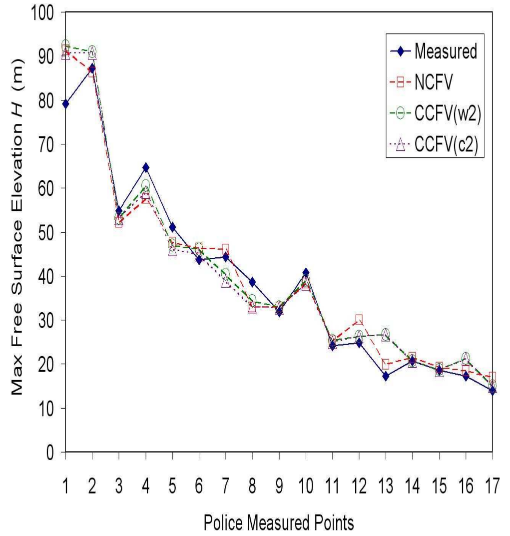

The Maplasset dam-break test case (EDF grid, CFL=0.9, $n_m = 0.033$)

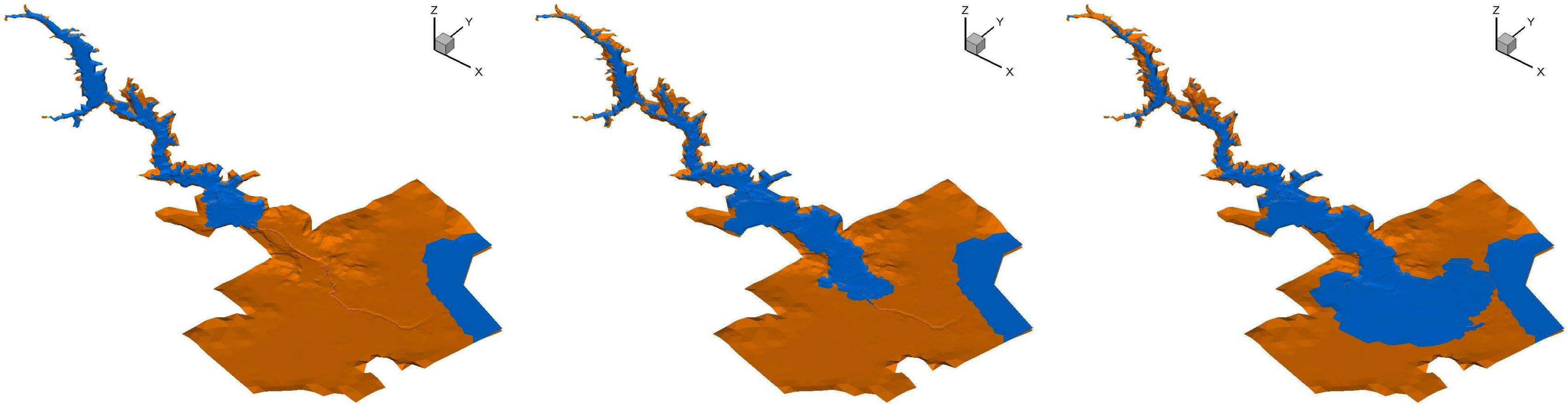

Water depth evolution at t=800s, 1600s, 2400s

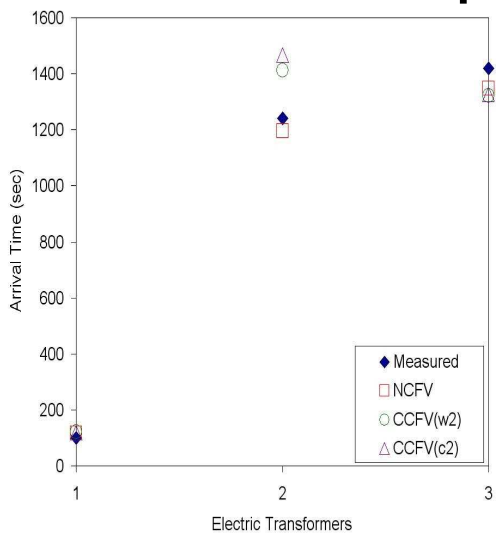

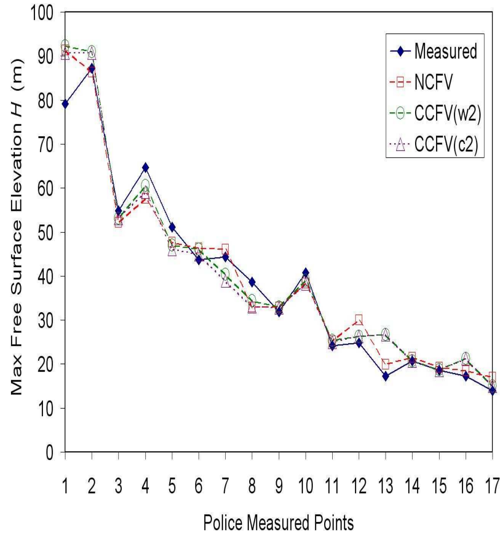

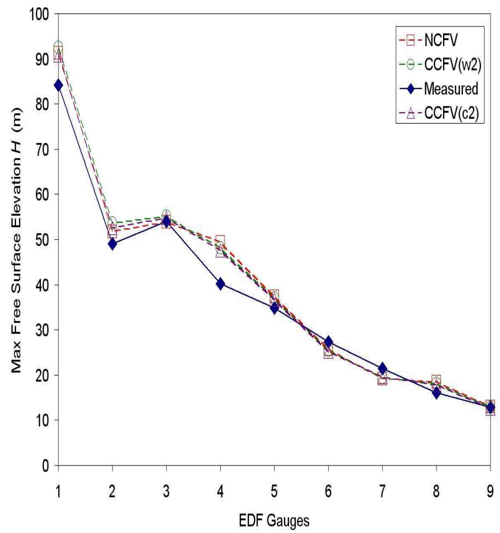

The Maplasset dam-break test case (EDF grid, CFL=0.9, $n_m = 0.033$)

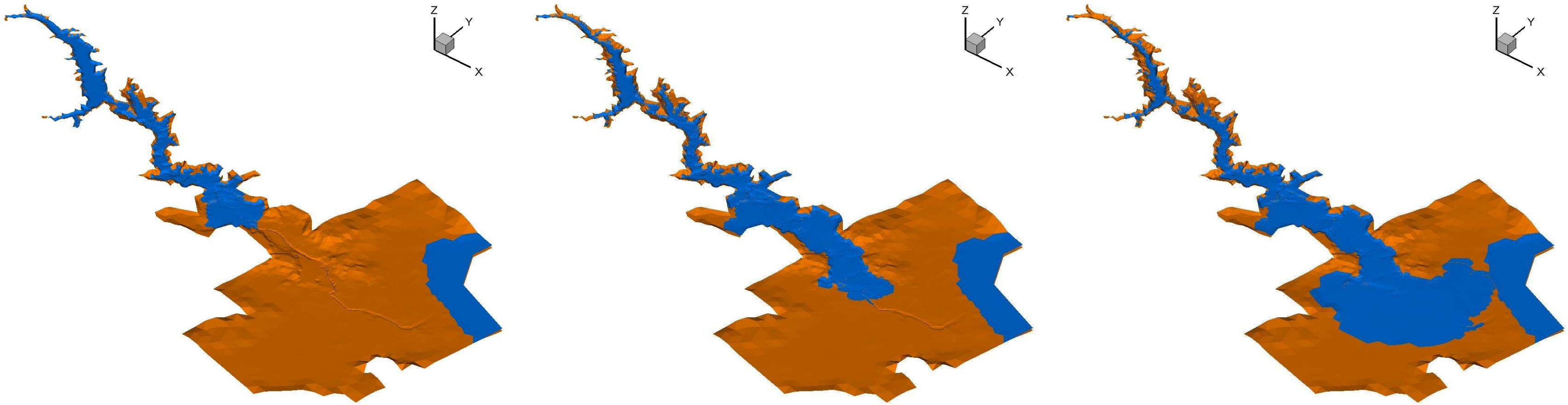

Water depth evolution at t=800s, 1600s, 2400s

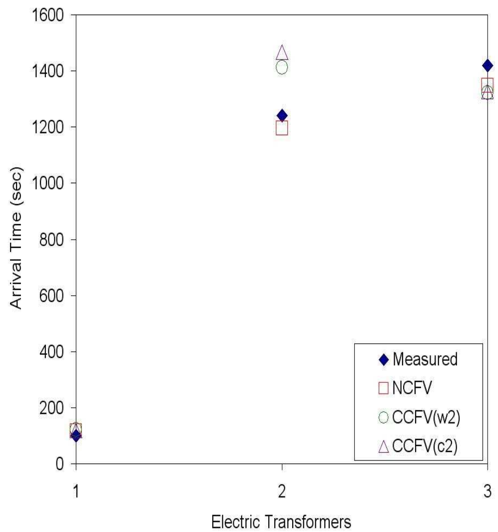

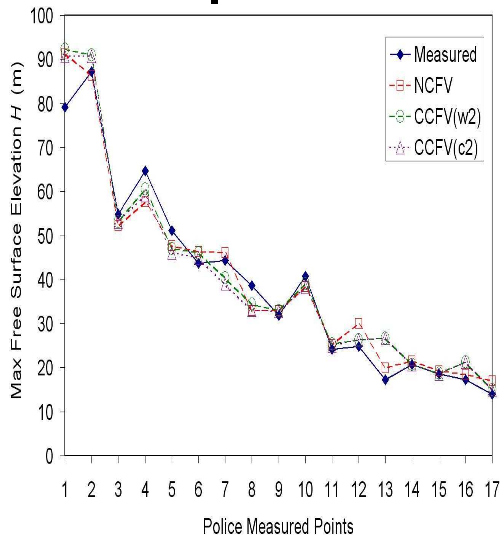

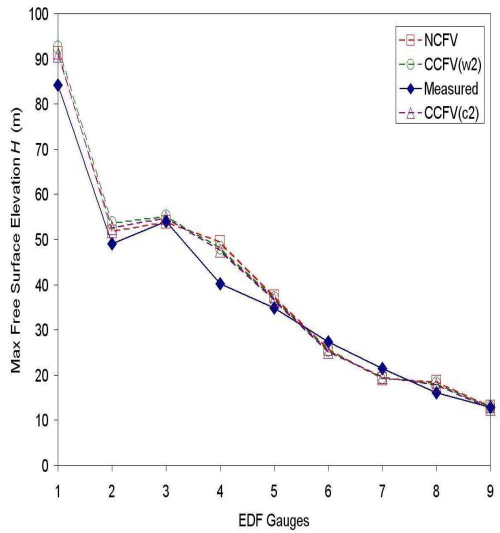

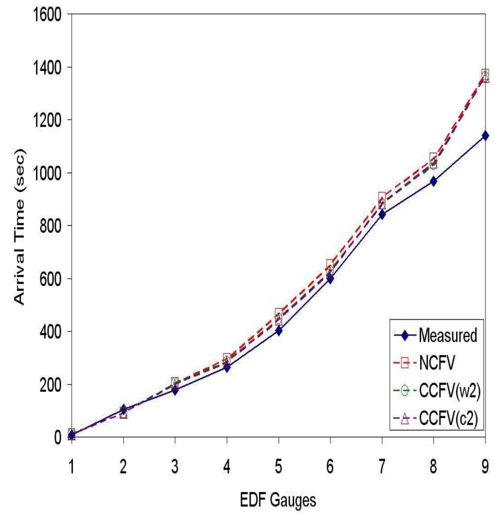

CONCLUSIONS

- The NCFV scheme exhibited identical convergence behavior on all grids.

CONCLUSIONS

- The NCFV scheme exhibited identical convergence behavior on all grids.
- For the CCFV approach different convergence behavior is exhibited (with an order reduction) for grids where the center of the face does not coincide with the reconstruction location.

CONCLUSIONS

- The NCFV scheme exhibited identical convergence behavior on all grids.
- For the CCFV approach different convergence behavior is exhibited (with an order reduction) for grids where the center of the face does not coincide with the reconstruction location.

  - The proposed correction for the reconstruction values remedies the problem (for both the compact and wide stencil G-G gradient computations)

CONCLUSIONS

- The NCFV scheme exhibited identical convergence behavior on all grids.
- For the CCFV approach different convergence behavior is exhibited (with an order reduction) for grids where the center of the face does not coincide with the reconstruction location.
  - The proposed correction for the reconstruction values remedies the problem (for both the compact and wide stencil G-G gradient computations)
  - For the wide stencil similar consistent convergence behavior to the NCFV is exhibited

CONCLUSIONS

- The NCFV scheme exhibited identical convergence behavior on all grids.
- For the CCFV approach different convergence behavior is exhibited (with an order reduction) for grids where the center of the face does not coincide with the reconstruction location.
  - The proposed correction for the reconstruction values remedies the problem (for both the compact and wide stencil G-G gradient computations)
  - For the wide stencil similar consistent convergence behavior to the NCFV is exhibited
  - Convergence to steady-state solutions is greatly improved.

CONCLUSIONS

- The NCFV scheme exhibited identical convergence behavior on all grids.
- For the CCFV approach different convergence behavior is exhibited (with an order reduction) for grids where the center of the face does not coincide with the reconstruction location.
  - The proposed correction for the reconstruction values remedies the problem (for both the compact and wide stencil G-G gradient computations)
  - For the wide stencil similar consistent convergence behavior to the NCFV is exhibited
  - Convergence to steady-state solutions is greatly improved.
- The effect of the grid's geometry at the boundary can lead to order reduction for the CCFV schemes (if the the center of the face does not coincide with the reconstruction location), even for good quality grids
  - Results with the wide stencil CCFV scheme exhibited, in general, better accuracy.

CONCLUSIONS

- The NCFV scheme exhibited identical convergence behavior on all grids.
- For the CCFV approach different convergence behavior is exhibited (with an order reduction) for grids where the center of the face does not coincide with the reconstruction location.
  - The proposed correction for the reconstruction values remedies the problem (for both the compact and wide stencil G-G gradient computations)
  - For the wide stencil similar consistent convergence behavior to the NCFV is exhibited
  - Convergence to steady-state solutions is greatly improved.
- The effect of the grid's geometry at the boundary can lead to order reduction for the CCFV schemes (if the the center of the face does not coincide with the reconstruction location), even for good quality grids
  - Results with the wide stencil CCFV scheme exhibited, in general, better accuracy.
- Both FV approaches to wetting and drying situations lead to order reduction but this drop is moderate and within acceptable limits
  - Important differences observed between the wetting and drying phase, with the results in

the drying phase being of reduced accuracy for the velocity computations

the drying phase being of reduced accuracy for the velocity computations

- For the friction treatment an order reduction for the velocity components was observed proportional to the implicitness introduced to the numerical treatment

the drying phase being of reduced accuracy for the velocity computations

- For the friction treatment an order reduction for the velocity components was observed proportional to the implicitness introduced to the numerical treatment
- For the Malpasset case, all formulations produced results close to field measurements, but with the NCFV scheme using half the degrees of freedom of the CCFV ones.

the drying phase being of reduced accuracy for the velocity computations

- For the friction treatment an order reduction for the velocity components was observed proportional to the implicitness introduced to the numerical treatment
- For the Malpasset case, all formulations produced results close to field measurements, but with the NCFV scheme using half the degrees of freedom of the CCFV ones.

References

- A.I. Delis, I.K. Nikolos and M.Kazolea, "Performance and comparison of cell-centered and node-centered unstructured finite volume discretizations for shallow water free surface flows", Archives of Computational Methods in Engineering, (accepted).
- I.K. Nikolos and A.I. Delis, "An unstructured nod-centered finite volume scheme for shallow water flows with wet/dry front over complex topography", Comput. Methods Appl. Mech. Engrg., 198:3723, 2009.

THANK YOU FOR YOUR ATTENTION!

2D steady-state with topography and friction

Known analytical solution, Murillo et al., 2007.

Start from water at rest, $n_m = 0.3$ and impose sub and super-critical boundary conditions

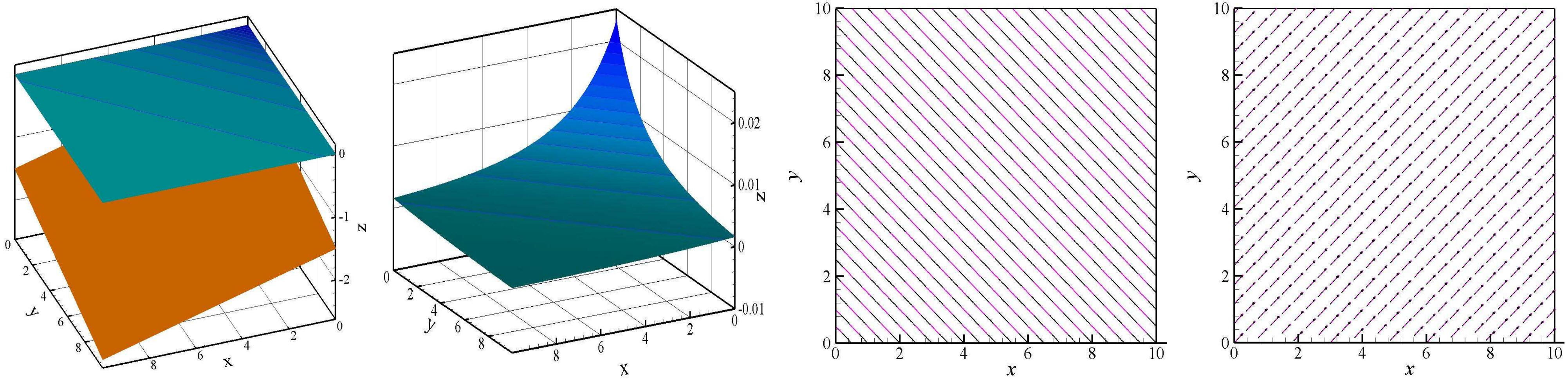

Compare explicit, semi-implicit and implicit friction term treatment (in terms of convergence rates)

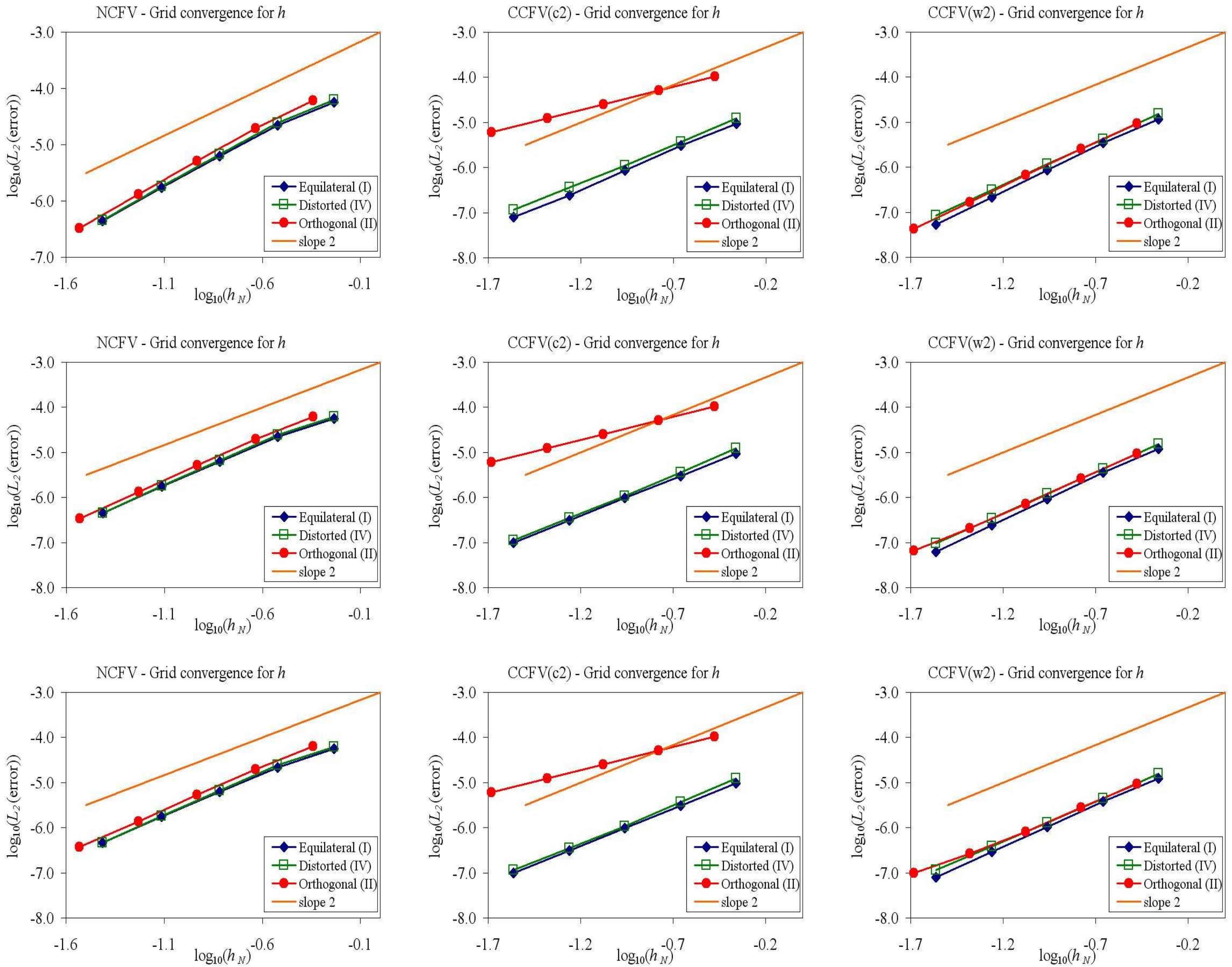
NCFV - Grid convergence for h
CCFV(c2) - Grid convergence for h
CCFV(w2) - Grid convergence for h
-3.0
-4.0
-5.0
-6.0
-7.0
-8.0
$\log_{10}(L_2(\text{error}))$
-1.6
-1.1
-0.6
-0.1
-1.7
-1.2
-0.7
-0.2
$\log_{10}(h_N)$
Equilateral (I)
Distorted (IV)
Orthogonal (II)
slope 2
NCFV - Grid convergence for h
CCFV(c2) - Grid convergence for h
CCFV(w2) - Grid convergence for h
NCFV - Grid convergence for h
CCFV(c2) - Grid convergence for h
CCFV(w2) - Grid convergence for h

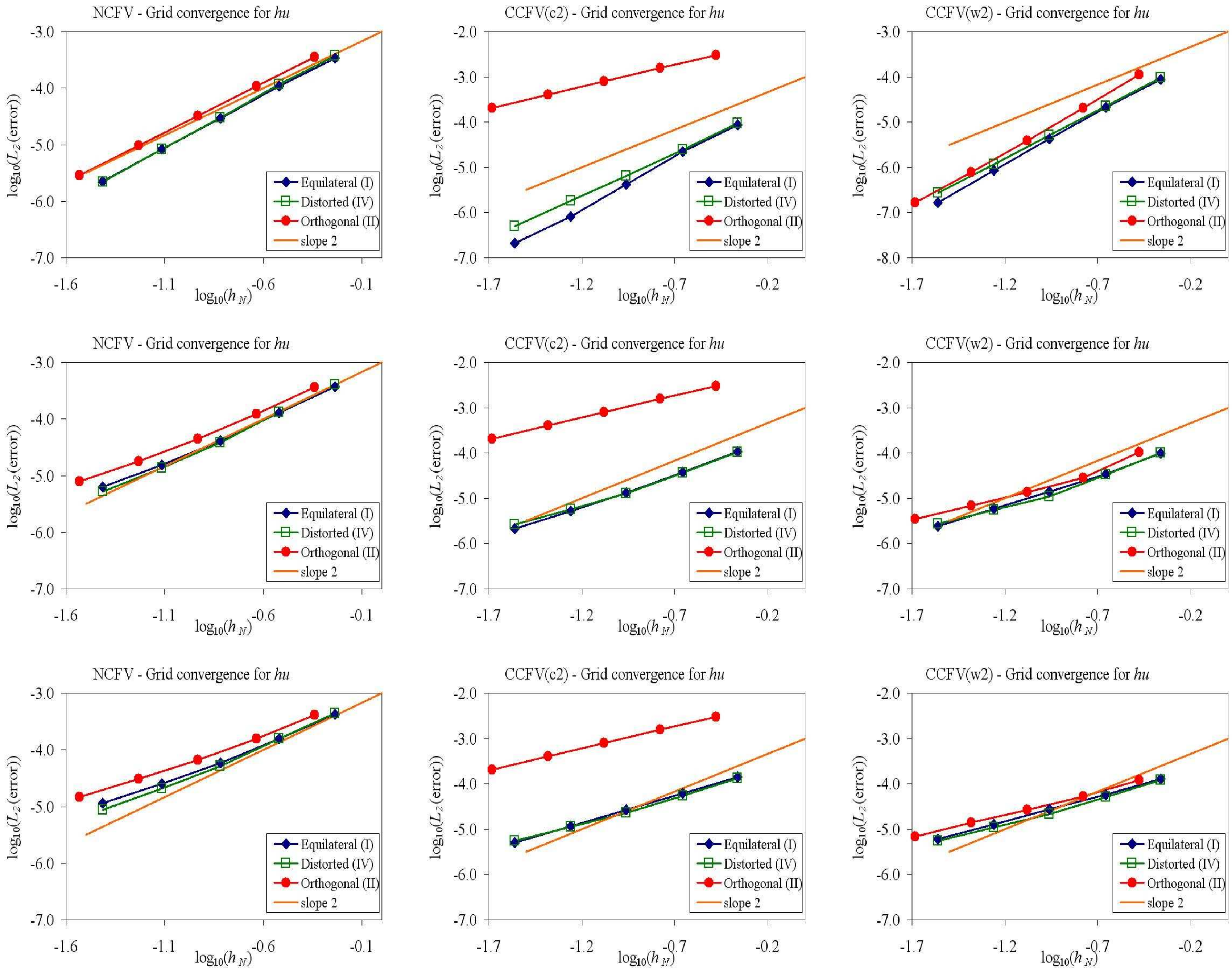
NCFV - Grid convergence for hu
CCFV(c2) - Grid convergence for hu
CCFV(w2) - Grid convergence for hu
NCFV - Grid convergence for hu
CCFV(c2) - Grid convergence for hu
CCFV(w2) - Grid convergence for hu
NCFV - Grid convergence for hu
CCFV(c2) - Grid convergence for hu
CCFV(w2) - Grid convergence for hu
log10(L2(error))
log10(hN)
Equilateral (I)
Distorted (IV)
Orthogonal (II)
slope 2